

**Study of Gas Permeability and Separation Behaviour for Removal of
High Content CO₂ from CH₄ by Using Membrane Modelling**

By

Lim Chin Han

Dissertation submitted in partial fulfilment of
The requirements for the
Bachelor of Engineering (Hons)
(Chemical Engineering)

January 2004

Universiti Teknologi PETRONAS
Bandar Seri Iskandar
31750 Tronoh
Perak Darul Ridzuan

€

7P

156

545

H233

2004

1) Separation Technology

CERTIFICATION OF APPROVAL

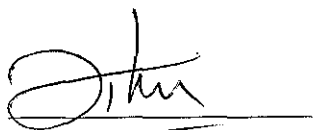
**Study of Gas Permeability and Separation Behaviour for Removal of High
Content CO₂ from CH₄ by Using Membrane Modelling**

by

Lim Chin Han

A project dissertation submitted to the
Chemical Engineering Programme
Universiti Teknologi PETRONAS
in partial fulfilment of the requirement for the
BACHELOR OF ENGINEERING (Hons)
(CHEMICAL ENGINEERING)

Approved by.



(Dr. Hilmi Bin Mukhtar)

Project Supervisor

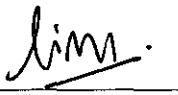
Universiti Teknologi PETRONAS

Tronoh, Perak

January 2004

CERTIFICATION OF ORIGINALITY

This is to certify that I am responsible for the work submitted in this project, that the original work is my own except as specified in the references and acknowledgements, and that the original work contained herein have not been undertaken or done by unspecified sources or persons.

A handwritten signature in cursive script, appearing to read 'lim.', is written above a horizontal line.

Lim Chin Han

ABSTRACT

The removal of CO₂ from natural gas down to the pipeline quality is an important step before the natural gas can be sold to the end users. Typical natural gas treatment's specification requires that the composition of CO₂ in the treated gas cannot be more than 2 mole%. Currently, amine scrubbing units like Benfield process is extensively used to treat low content of CO₂ in the natural gas. For high concentration of CO₂ in the natural gas stream, the use of amine unit is economically restricted, as the recirculation rate needs to be increased to cater the need. The use of membrane separator to treat high content CO₂ natural gas has matured over the years and is said to work best at high CO₂ inlet partial pressure, as this results in increased permeation of the acid gas across the membrane. However, in the meantime to achieve low sale gas specification, the natural gas recovery in a membrane separator remains a question that needs to be explored.

This modelling work comprises the study of gas permeability of pure CO₂ and CH₄ and the separation behaviour of CO₂ / CH₄ mixture under different process influences. The purpose is to predict the capability of membrane separator in separating high content CO₂ in the natural gas by using mathematical modelling. Data for γ -alumina and acetate cellulose membranes, as cited from various references were used in this modelling work. The accuracy of the models developed, which incorporates the main transport mechanisms due to viscous, Knudsen and surface diffusion, was tested using experimental data cited.

Simulation results show that the permeability of CO₂ and CH₄ depend strongly on the pore size of the membrane, temperature and feed composition of the mixture. The effect of pressure on gas permeability is only apparent at small pore size.

It was found that surface diffusion predominates the other transport mechanisms at small pores, and it poses the most selective transport mechanism to separate the CO₂ from CH₄. However, when the pore size increases, surface diffusion starts to lose its effect as the gas molecules continue to diffuse via Knudsen diffusion mechanism. The results showed that Knudsen diffusion eventually increases the permeability of

the gas molecules, but sacrifice in term of separation selectivity was observed at higher pore size. The contribution of viscous diffusion is not apparent as overall.

The permeability of pure gas is inversely proportional to the system temperature, and directly proportional to the operating pressure at small pores only. The variation of surface diffusion due to the effects of both pressure and temperature is profound at small pore regions. The permeability of CO₂ and CH₄ in CO₂ / CH₄ mixture will approach the pure gas permeability as their feed composition increases.

The investigation of separation behaviour of this binary system revealed that the performance of the single – stage alumina membrane separator is constant over a range of possible operating pressures. However, the separation factor decreases when the temperature increases. It showed that the separation factor of this binary system can be enhanced to be maximum at temperature near 80°C for separation that takes place in small pore region of the γ -alumina membrane used. The separation factor is also a strong function of both the feed composition of CO₂ and the separation stage cut. Membrane separator becomes more efficient in term of selectivity and removal efficiency at high feed composition of CO₂ and higher stage cut. The high stage cut used to obtain sharp separation, however decreases the attractiveness of this binary separation due to increased loss of natural gas to the impurities stream.

ACKNOWLEDGEMENT

The author deeply feels that the accomplishment of this endeavour would not be that successful without endless host of help and support from the following personnel. First and foremost, the author would like to thank his beloved parents and brothers for their continuous support and motivation. They were source of inspiration whenever the project seemed to hit the rock bottom.

Sincere gratitude would like to be directed to Dr. Hilmi Bin Mukhtar, the author's project supervisor in realising this project. The result of this study would not be fruitful and meaningful without his motivation, patience, constructive comments and the precious time he spent to discuss the project proper throughout the four – month project period.

The author would also like to thank fellow expatriates Mr. Benjamin P. Manoloto and Mr. Shyam Goyal, both contract employees in PETRONAS Penapisan Melaka for their vivid inputs to the project paper. It was no waste of effort in writing long mails to consult them, as the replies seen were especially meaningful to the success of this project.

The effort shown by the author's fellow colleagues, Ms. Nun Zuraini Zailaini and Ms. Marcella Abdul Karim was deemed as the backbone to the success of this project. They were determined and resourceful in seeking necessary information for the project proper and their suggestions during every discussion contributed very much to this project.

Last but not least, the author would like to direct his appreciation to lecturers from Universiti Teknologi PETRONAS, lab technicians and fellow friends for their support throughout the project period. Each of these individuals showed no reluctance whenever the author needed their help in accomplishing this project.

CONTENTS

CERTIFICATION OF APPROVAL	i
CERTIFICATION OF ORIGINALITY	ii
ABSTRACT	iii
ACKNOWLEDGEMENT	v
LIST OF ILLUSTRATION	viii
ABBREVIATIONS AND NOMENCLATURES	xi
CHAPTER 1: INTRODUCTION	1
1.1 Background of Study – Membrane Separation	1
1.1.1 Gas Separation Using Membrane.....	1
1.1.2 Membrane Materials	3
1.2 Carbon Dioxide in Natural Gas.....	4
1.2.1 Removal of CO ₂	5
1.3 Problem Statement	9
1.4 Objectives and Scope of Study	10
1.4.1 Objectives.....	10
1.4.2 Scope of study	10
CHAPTER 2: LITERATURE REVIEW	11
2.1 Important Concepts	11
2.2 Pore Characteristics and Membrane Architecture.....	13
2.3 Gas Permeability Model.....	14
2.4 Works on Flow Model by Others.....	17
CHAPTER 3: THEORY	21
3.1 Gas Transport in Porous Material	21
3.1.1 Viscous Diffusion	22
3.1.2 Gas Diffusion	23
3.1.3 Surface Diffusion	26
3.1.4 Capillary Condensation.....	28
3.2 Gas Permeability as An Integration of All Transport Mechanism.....	29

3.3 Permeability of Gas in Mixture.....	31
3.4 Separation Factor	32
3.5 Complete Mixing Model.....	33
CHAPTER 4: METHODOLOGY	35
4.1 Model Development.....	35
4.1.1 Assumptions in Model Development.....	35
4.1.2 Basic Equations Used.....	35
4.1.3 Features of the Models	36
4.2 Software Required.....	36
4.3 Membrane Properties	37
CHAPTER 5: RESULTS AND DISCUSSION.....	40
5.1 Mechanisms of Flow of Gas Molecules in Porous Membrane	40
5.1.1 Effect of Pore Size on Gas Permeability.....	40
5.1.2 Effect of Operating Pressure on Gas Permeability	43
5.1.3 Effect of Temperature on Gas Permeability.....	46
5.2 Pure Gas Permeability Versus Permeability of Gases in Binary Mixture	48
5.3 Separation of CO ₂ / CH ₄ Binary System for High CO ₂ Concentration	51
5.3.1 Effect of Operating Pressure and Pore Size on Separation Factor.....	51
5.3.2 Effect of Feed Concentration on Separation Factor.....	52
5.3.3 Effect of Stage Cut on Separation Factor.....	53
5.3.4 Effect of Temperature on Separation Factor.....	54
5.3.5 Pipeline Quality of the Sale Gas	56
5.4 Model Validation	59
CHAPTER 6: CONCLUSION AND RECOMMENDATION	62
6.1 Conclusion	62
6.2 Recommendations.....	65
REFERENCES.....	68
Appendix A: Properties of CO ₂ and CH ₄	72
Appendix B: Compressibility factors of CO ₂	73
Appendix C: Compressibility factors of CH ₄	74
Appendix D: Lennard – Jones parameters for CO ₂ (Bird <i>et al.</i> , 1960).....	75
Appendix E: Lennard – Jones parameters for CH ₄ (Bird <i>et al.</i> , 1960)	76
Appendix F: Mathcad Programming Samples	77

LIST OF ILLUSTRATION

- Figure 1.1 Membrane process for gas separation.
- Figure 2.1 Schematic diagram of different types of pores in a porous solid. A: Isolated pore; B, F: dead end pores; C, D: Tortuous / rough pores; E: Conical pore.
- Figure 2.2 Schematic representation of Dusty Gas Model.
- Figure 2.3a Complete mixing model.
- Figure 2.3b Cross – flow model.
- Figure 2.3c Counter – current flow model.
- Figure 2.3d Co – current flow model.
- Figure 3.1a Viscous diffusion.
- Figure 3.1b Knudsen diffusion.
- Figure 3.1c Surface diffusion.
- Figure 3.1d Capillary condensation.
- Figure 3.2 Cross sectional view of collision in the pore.
- Figure 3.3 Detailed process flow for complete mixing model.
- Figure 4.1 Algorithm to solve the model for both pure gas permeability and permeability of gas specie in a mixture.
- Figure 4.2 Algorithm to solve the model to compute the separation factor for CO₂ – CH₄ separation.
- Figure 5.1 Effect of pore size on the mechanisms of flow for pure CO₂ in γ -alumina membrane at T=303 K, P=60 atm.
- Figure 5.2 Effect of pore size on the mechanisms of flow for pure CH₄ in γ -alumina membrane at T=303 K, P=60 atm.
- Figure 5.3 Effect of pore size on total permeability of CO₂ and CH₄ in γ -alumina membrane at T=303 K, P=60 atm.
- Figure 5.4 Effect of pressure on mechanism of flow for CO₂ in γ -alumina membrane at T=303 K, $r_p=0.2$ nm.

- Figure 5.5 Effect of operating pressure on total permeability of CO₂ at different pore sizes in γ -alumina membrane at T=303 K.
- Figure 5.6 Effect of operating pressure on total permeability of CH₄ at different pore sizes in γ -alumina membrane at T=303 K.
- Figure 5.7 Effect of temperature on mechanism of flow for CH₄ in γ -alumina membrane at P=60 atm.
- Figure 5.8 Effect of temperature on total permeability of CH₄ at different pore sizes in γ -alumina membrane at P=60 atm.
- Figure 5.9 Effect of temperature on total permeability of CO₂ at different pore sizes in γ -alumina membrane at P=60 atm.
- Figure 5.10 Pure gas permeability versus permeability of gas in mixture (20% CO₂ – 80% CH₄) in γ -alumina at $r_p=0.2$ nm, T=303 K.
- Figure 5.11 Pure gas permeability versus permeability of gas in mixture (20% CO₂ – 80% CH₄) in γ -alumina at $r_p=2$ nm, T=303 K.
- Figure 5.12 Gas permeability of CO₂ in CO₂ / CH₄ mixture as a function of feed composition at different pore size in γ -alumina membrane at P=60 atm, T=303 K.
- Figure 5.13 Gas permeability of CH₄ in CO₂ / CH₄ mixture as a function of feed composition at different pore size in γ -alumina membrane at P=60 atm, T=303 K.
- Figure 5.14 Effects of feed pressure on separation factor for CO₂ – CH₄ separation in γ -alumina at different pore sizes, T=303 K, $x_f=0.30$, $\theta=0.206$.
- Figure 5.15 Effects of feed concentration on separation factor for CO₂ – CH₄ separation as a function of pressure ratio in γ -alumina at T=303 K, $r_p=0.2$ nm $\theta=0.206$.
- Figure 5.16 Effects of stage cut on separation factor for CO₂ – CH₄ separation as a function of pressure ratio in γ -alumina at T=303 K, $x_f=0.30$, $r_p=0.2$ nm.
- Figure 5.17 Effect of operating temperature on separation factors for CO₂ – CH₄ separation in γ -alumina at different pore sizes, P=60 atm, $x_f=0.30$.
- Figure 5.18 Effects of feed concentration on separation factor for CO₂ – CH₄ separation as a function of temperature in γ -alumina at P=60 atm, $r_p=0.2$ nm $\theta=0.206$.

Figure 5.19	Variation of y_{pCO_2} and x_{oCO_2} as a function of feed composition of CO_2 in separation of $CO_2 - CH_4$ in γ -alumina membrane at $T=303$ K, $P=60$ atm, stage cut=0.206.
Figure 5.20	Variation of y_{pCO_2} and x_{oCO_2} as a function of feed composition of CO_2 in separation of $CO_2 - CH_4$ in γ -alumina membrane at $T=303$ K, $P=60$ atm, stage cut=0.706.
Figure 5.21	% removal of CO_2 and % loss of CH_4 at different stage cuts as a function of feed composition of CO_2 in $CO_2 - CH_4$ separation in γ -alumina membrane at $T=303$ K, $P=60$ atm.
Figure 5.22	Comparison between model prediction and experimental data for CO_2 permeability on acetate cellulose membrane at $T=305$ K, stage cut=0.178, $x_f=0.5$
Figure 5.23	Comparison between model prediction and experimental data for CO_2 / CH_4 separation factor on acetate cellulose membrane at $T=305$ K, stage cut=0.178, $x_f=0.5$
Table 1.1	Worldwide membrane market size.
Table 1.2	Materials for gas separating membranes (Freeman and Pinnau, 1999).
Table 1.3	Producer of membrane material (Othman, 2001).
Table 1.4	Composition of CO_2 in some natural gas wells (Rojey <i>et al.</i> , 1997).
Table 1.5	Pipeline quality of treated natural gas.
Table 1.6	Comparison of absorption and membrane for CO_2 removal (Echt, 2002).
Table 2.1	Transport regimes in porous membranes.
Table 4.1	Properties of γ -alumina and acetate cellulose membrane.

ABBREVIATIONS AND NOMENCLATURES

A_m	=	area of membrane. [m^2]
C_g	=	concentration of gas. [$mol.L^{-1}$]
C_s	=	concentration of gas molecules adsorbed onto the surface. [$mol.L^{-1}$]
\bar{c}	=	velocity of gas. [$m.s^{-1}$]
D_e	=	effective diffusivity. [$m^2.s^{-1}$]
D_i	=	ordinary gas diffusion for i. [$cm^2.s^{-1}$]
$D_{i,mix}$	=	ordinary diffusion of gas in a mixture. [$m^2.s^{-1}$]
$D_{k,i}$	=	knudsen diffusion for i. [$cm^2.s^{-1}$]
D_s	=	surface diffusion. [$cm^2.s^{-1}$]
f	=	equilibrium loading factor. [$m^3.kg^{-1}$]
J_T	=	total effective flux of the gas molecules. [$mol.m^{-2}.s^{-1}$]
L_m	=	length of the cylindrical pore. [m]
M_i	=	molecular weigh of gas specie i. [$g.mol^{-1}$]
\bar{P}	=	average pressure across the membrane. [atm]
P'_i	=	permeability of i. [$mol.s.kg^{-1}$]
P_r	=	ratio of permeate pressure divided by the feed pressure. [-]
p_h	=	high-pressure side. [atm]
p_l	=	low-pressure side. [atm]
ΔP	=	pressure drop across the membrane. [atm]
q_A	=	flow rate of A in permeate. [$cm^3(STP).s^{-1}$]
q_f	=	total feed flow rate. [$cm^3(STP).s^{-1}$]
q_o	=	outlet reject flow rate. [$cm^3(STP).s^{-1}$]
q_p	=	permeate flow. [$mol.s^{-1}$]
R	=	universal gas constant. [$82.06cm^3.atm.mol^{-1}.K^{-1}$]
R_m	=	radius of cylindrical pore. [m]
r_p	=	pore radius. [m]
T	=	temperature. [K]
t_m	=	thickness of membrane. [m]

x_o	=	reject mole fraction. [-]
y	=	mole fraction at the permeate side. [-]
y_p	=	permeate mole fraction. [-]
Z	=	North-South axis.
ε	=	porosity of the membrane. [-]
η	=	shape factor of the membrane. [-]
μ_i	=	viscosity of gas i. [kg.m ⁻¹ .s ⁻¹]
$\mu_{i,mix}$	=	average viscosity for the gas mixture. [kg.m ⁻¹ .s ⁻¹]
λ	=	mean free path of travel of gas molecules in the pore. [m]
τ	=	tortuosity factor of the membrane. [-]
σ^2, Ω_μ	=	Lennard-Jones parameters as available in Bird et al. (1960)

CHAPTER 1

INTRODUCTION

1.1 Background of Study – Membrane Separation

In a membrane separation process, a feed consisting of a mixture of two or more components is partially separated by means of a semi permeable barrier (the membrane) through which one or more species move faster than another or other species. Although the feed is usually liquid or gas, the membrane separator is capable to handle solid (Seader and Henley, 1998). The barrier is most often a thin, nonporous polymeric film, but may also be porous polymer, ceramic, or metal materials, or even a liquid or gas. It is utmost important to make sure that the barrier does not dissolve, disintegrate or break in the membrane separator.

1.1.1 Gas Separation Using Membrane

In 1831, J. V. Mitchell reported for the first time that gases permeated through rubber membranes and that the flux of each gas was different (Osada and Nakagawa, 1992). At that time, very few polymer membranes had high gas permeability and excellent separation properties. In the early 1950s, research concerning the separation of helium from natural gas or oxygen enrichment from air was begun. As the technology for synthesis of polymers has progressed, many new materials for practical gas separations have been developed (Osada and Nakagawa, 1992).

The membrane process of a typical gas separation system is shown in Figure 1.1 where the feed mixture is separated into a retentate stream and permeate stream. Retentate is the stream where the species does not pass through the barrier, and thus is retained whereas permeate consists of the part of stream that does pass through the membrane. In gas separations such as removal of CO₂ and H₂S from natural gas, the retentate stream consists of the purified gas (natural gas) whereas the permeate

stream contains the impurities removed (CO_2 , H_2S , etc.). The gas carrier is usually a liquid or gas used to help to remove the permeate.

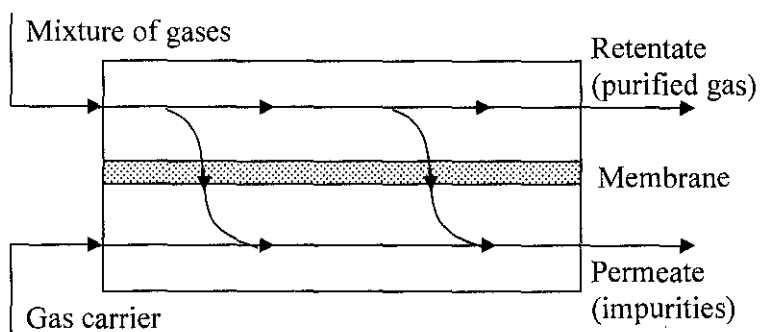


Figure 1.1: Membrane process for gas separation.

Large – scale application of membrane gas separations was in rapid development since 5 decades ago. In 1979, Mosanto Chemical Company introduced a hollow – fibre membrane of polysulfone to separate certain gas mixtures – for example, to enrich hydrogen – and carbon dioxide – containing streams (Seader and Henley, 1998). Membrane gas separation had since become economically viable to conventional separation processes such as absorption, evaporation and distillation. The vast fraction of the present – day usage of membranes – nitrogen removal from air, hydrogen recovery and upgrading, synthesis gas ratio adjustment, acid gas removal from natural gas, moisture removal from hydrocarbon streams and vent stream cleanup – will remain in the workhorse applications in the future.

Membrane gas separation must compete with distillation at cryogenic condition, absorption and pressure – swing adsorption. The uses of membranes in gas separation offer several advantages. As cited by Spillman and Sherwin (1990), are low capital investment, ease of installation, ease of operation, absence of rotating parts, high process flexibility, low weight and space requirement, and low environmental impact. In addition, if the feed gas is already at so high a pressure that a gas compressor is not needed, then no utilities are required. As a result, application of membranes in gas separation should continue to expand rapidly in the next decade.

The market size of membrane gas separation industry worldwide is growing rapidly. It was observed that the worldwide membrane market size had multiplied as much as 75 times over a 10 – year span from 1986 to 1996 (Hsieh, 1996). Table 1.1 shows the breakdown of market size of the four major membrane – based processes in 1996. This data, however, highlights the growing importance of membrane gas separation application in the industry.

Table 1.1: Worldwide membrane market size (Hsieh, 1996).

Process	Major Applications	1986 Sales	1996 Sales
Microfiltration	Biotechnology, chemicals, electronics, environmental control, food and beverage, pharmaceutical	\$ 550 mil.	\$ 1.5 bil.
Ultrafiltration	Biotechnology, chemicals, environmental control, food and beverage	\$ 350 mil.	\$ 1.1 bil.
Reverse Osmosis	Desalinating sea water, electronics, food and beverage	\$ 120 mil.	\$ 530 mil.
Gas Separation	Environmental control	\$ 20 mil.	\$ 1.5 bil.

1.1.2 Membrane Materials

The membrane gas separation industry is so far dominated by polymeric membranes, which consists of natural polymers and synthetic polymers. Natural polymers include wool, rubber, and cellulose. A wide variety of synthetic polymers has been developed and commercialised since 1930. The emergence of inorganic membrane materials such as ceramics and metal membrane has brought not little attention in the R&D field of membrane separations. Table 1.2 and 1.3 list some common membrane materials used for gas separation and producers of membrane material.

Table 1.2: Materials for gas separating membranes (Freeman and Pinnau, 1999).

Organic	Industrial Application
Polysulfone, Polyethersulfone	Separation of H ₂ / CH ₄ , CO ₂ / CH ₄ , H ₂ S / CH ₄
Celluloseacetate	Separation of CO ₂ / CH ₄ , N ₂ / O ₂ , H ₂ / CH ₄
Inorganic	
Carbon Molecular Sieves	Separation of H ₂ O / natural gas, N ₂ / CH ₄
Zeolites	Separation of H ₂ O / CH ₄ , O ₂ / N ₂ , He / C ₂ H ₆
Metal	
Palladium	Separation of H ₂ / N ₂
Titania	Separation of H ₂ / N ₂ , N ₂ / O ₂

Table 1.3: Producer of gas separation membrane material (Othman, 2001).

No.	Company Name	Type of Membrane
1	Five Continents USA Corporation, USA	Organic and Inorganic
2	NGK Insulators Ltd., Chemical Apparatus Division, Japan	Organic and Inorganic
3	Millipore Corporation, USA	Organic and Inorganic
4	Koch Membrane Systems, Singapore	Organic and Inorganic
5	C.N.C.E, China	Organic and Inorganic
6	VELTEROP Ceramic Membrane Technology, the Netherlands	Organic and Inorganic
7	US Filter Ceramique Industrielles, France	Organic and Inorganic
8	Divex, Great Britain	Organic and Inorganic

Polymeric membranes are most cost attractive in gas separation when operated at low operating temperature range. They are known for their good sorptivity of certain gas species and thus making the separation more selective. On the other hand, inorganic membranes and metal offer some advantages in term of operation at severe temperature and pressure. They are generally chemically stable and can withstand severe operating conditions. However, Freeman and Pinnau (1999) pointed out that inorganic membranes and metal have no significant market share in the future due to its high price and difficulties during reproducible large – scale production.

1.2 Carbon Dioxide in Natural Gas

Carbon Dioxide (CO₂) is a well – known acid gas that is present in the natural gas. In enhanced oil recovery (EOR) application, the gas is pumped into depleting oil reserves at high pressures to drive residual oils to existing oil wells. Over an extended period of time, the CO₂ gas mixes with the natural gas associated with the wells and can reach as high as 95% (Spillman, 1989). The composition of CO₂ in the existing natural gas wells varies for different geographical locations. Its composition can reach as high as 80% in certain natural gas wells (Rojey *et al.*, 1997). Table 1.4 shows the composition of CO₂ in some natural gas wells in the world.

Table 1.4: Composition of CO₂ in some natural gas wells (Rojey *et al.*, 1997).

No.	Location	Composition (%)
1	Lacq, France	9.3
2	Frigg, Norway	0.3
3	Uch, Pakistan	46.2
4	Kapuni, New Zealand	43.8
5	Uthmaniyah, Saudi Arabia	8.9
6	Terengganu, Malaysia	7.0
7	Krecsegopan, Poland	83.0
8	North German Plain, Germany	60.0
9	Kirkuk, Iraq	7.1
10	Duri, Indonesia	23.0

1.2.1 Removal of CO₂

Due to its acidic nature and being non – combustible, CO₂ in the natural gas must be removed to a permissible level. Typical pipeline quality states that the composition of CO₂ in the treated gas stream must not be more than 2% (Spillman, 1989). In Malaysia, Gas Malaysia set an even more stringent limit where the level of CO₂ is further reduced to about 1.8% maximum. Table 1.5 shows the typical pipeline quality of treated natural gas where the composition of CO₂ is highlighted.

Table 1.5: Pipeline quality of treated natural gas.

Component	Composition (%) *	Composition (%) **
CH ₄	93.60	92.73
C ₂ H ₆	3.00	4.07
C ₃ H ₈	0.50	0.77
C ₄₊	0.20	0.15
CO₂	2.00 (max)	1.83 (max)
He	0.06	Trace
H ₂	0.04	Trace
O ₂	Trace	Trace
Hg	Trace	Trace
N ₂	Trace	0.45
H ₂ S	Trace	Trace

* Data adopted from Spillman (1989).

** Data adopted from Gas Malaysia, 2003.

The main processes used for acid gas removal are based on absorption (Amine scrubbing and hot Potassium Carbonate scrubbing), and the selectivity of the solvent

with respect to acid gas is based on an affinity of the chemical or physical type. Membrane gas separation has a substantial potential, but, today, industrial applications are still limited (Rojey *et al.*, 1997). Text in the following sections illustrates more about the processes mentioned and their respective advantages and disadvantages will be outlined and discussed.

a. Amine and Potassium Carbonate Scrubbing

Amine scrubbing has been used to remove CO₂ from natural gas since long time ago. The most famous application is the Benfield scrubbing process, which is currently used in PGB, Malaysia. In CO₂ removal using amine, an aqueous alkanolamine solution is contacted in an absorber with natural gas containing CO₂. In the process, the basic amine reacts with the acidic CO₂ vapours to form a dissolved salt, allowing purified natural gas to exit the absorber. The rich amine solution is regenerated in a stripper column, concentrating the CO₂ into an acid gas stream. Lean solution is cooled and returned to the absorber so that the process is repeated in a closed loop.

Hot potassium carbonate scrubbing process is similar to an amine process, but the potassium carbonate solutions used are usually more concentrated (20 to 40%) than the amine solutions. This process was originally intended to remove CO₂, but H₂S is also absorbed (Arnold and Stewart, 1989). Absorption by a “hot” potassium carbonate solution considerably boosts the absorption rate of CO₂. In present day processes, the absorption and regeneration steps are carried out at similar temperatures (about 110°C), eliminating the heat exchanger between the rich and lean solutions. Increasing the temperature in the absorption step allows higher carbonate concentrations (Rojey *et al.*, 1997).

b. CO₂ Removal with membranes

Meyer *et al.* (1991) and Cooley (1990) reported that gas permeation is already applied industrially to remove CO₂ from natural gas. So far, these units have only been used for small capacities and they can be justified economically with commercially – available membranes only if the inlet CO₂ concentration is high (Johnston and King, 1987).

Membranes are currently used for CO₂ removal from natural gas processing at processing rates from 1 MMSCFD to 250 MMSCFD (Echt, 2002). New units are in design or construction to handle volumes up to 500 MMSCFD (Echt, 2002). It has been recognised for many years that non – porous polymer films exhibit a higher permeability toward some gases than towards others. The mechanism for gas separation is independent of membrane configuration and is based on the principle that certain gases permeate more rapidly than others.

Single – stage membrane units are recommended for low – flow applications while a recycle loop should be considered for higher flow rates to minimise the loss of hydrocarbons due to incomplete separation. Separation of carbon dioxide from hydrocarbon is most cost competitive at low flow rates, for high carbon dioxide concentrations or for offshore platforms (Hsieh, 1996). Organic membranes start to be applied in this application. To be competitive with organic membranes, the inorganic membranes need to provide higher separation factors and or higher permeability.

c. Performance of Absorption and Membranes

As mentioned in the preceding paragraphs that membranes were restricted to either small natural gas streams or those with very high CO₂ content, such as in enhanced oil recovery CO₂ floods. However, as the technology matures, the technology spreads into a wider variety of natural gas sweetening application. Now that the technology becomes better known, one can stand back and look at the relative strength and weaknesses of the process versus the more established absorption technology. Table 1.6 shows some key areas for comparisons between amine absorption and membrane gas separation.

There can be no hard and fast rules applied to the comparisons made in Table 1.6 because all CO₂ removal systems are, by nature, site specific. The systems differ according to the natural gas being processed, the location of the installation and the economic parameters used by the end customers. For instance, membrane systems can be easily installed on platform due to its lightweight for CO₂ removal in EOR CO₂ floods.

Table 1.6: Comparison of absorption and membrane for CO₂ removal (Echt, 2002).

Operating Issues		
	Absorption	Membranes
User comfort level	Very familiar	Still new
Hydrocarbon losses	Very low	Losses depend upon conditions
Meets low CO ₂ specs.	Yes (ppm levels)	No (<2% is economic challenging)
Energy consumption	Moderate to high	Low
Operating cost	Moderate	Low
Maintenance cost	Low to moderate	Low
Ease of operation	Relatively complex	Relatively simple
Environmental impact	Moderate	Low
Dehydration	Product gas saturated	Product gas dehydrated
Capital Cost Issue		
	Absorption	Membranes
Delivery time	Long for large systems	Modular construction is faster
On – site installation time	Long	Short for skid – mounted equipment
Pre – treatment	Low	Low to moderate
Recycle compression	Not used	Use depends upon conditions

Another consideration in comparison is the hydrocarbon recovery. Absorption units do lose some feed hydrocarbons due to solubility and entrainment problems. Typical losses are less than 1% of the feed gas. For single – stage membrane system, hydrocarbon losses can vary from 2% to 10% or even more, depending on the processing conditions (Echt, 2002). Multistage or recycle configurations are used to reduce the hydrocarbon loss. However, when the loss of hydrocarbon to the permeate stream can be neglected, the loss of hydrocarbon in the off gas stream can actually be used for fuel gas, like a direct fired hot oil system heater, or be compressed for power generation using turbine.

The size of an amine (absorption) unit is directly related to the moles of CO₂ removed from the feed gas. As CO₂ content rises from low to moderate partial pressures in the feed, the rich solvent loading increases to somewhat offset the increased demand for solvent. When the partial pressures increase to high levels, the solvent approaches a maximum loading. Any increase in CO₂ can only be removed by increasing the circulation rate. The same is not true for membranes, as permeation

rate increases as the feed gas CO₂ partial pressure increases, making the membrane much more efficient at high CO₂ concentration. As shown in Table 1.6, single staged membrane will lose its efficiency in order to meet the low sales gas specifications, while amine scrubbing works very economically. Future technology suggests a combination of the technologies in series (Hybrid system) to treat gases with a high partial pressure of CO₂. Membrane will work where it is best (i.e. at high CO₂ partial pressure) whereas the solvent system works where it is best (i.e. achieving low specification for treated CO₂ content). More Illustrations regarding the development of the mentioned Hybrid system can be found in Echt (2002).

1.3 Problem Statement

The composition of CO₂ in natural gas may vary from 2 – 80% depending on the geographical location of the well. Due to its compactness and economic attractiveness, membrane gas permeation emerges as an effective alternative to the conventional absorption units. The removal of CO₂ is very important and the concentration of CO₂ must be below 2% before the gas can be sold. Gas Malaysia specifies an even more stringent level where a maximum 1.83% is to be achieved in the treated stream. In the meantime of achieving this low sales gas target, the problem of hydrocarbon recovery in the retentate stream arises. According to Echt (2002), the hydrocarbon losses in a single staged membrane system can vary from 2 to 10% or even more depending on the various process parameters. This causes the single staged membrane system to lose its economic justification despite being efficient to handle the high content CO₂ natural gas stream.

Mathematical models are very helpful in understanding the mechanism of permeation and separation behaviour for high content CO₂ removal as a function of various process influences. Furthermore, the similar empirical study carried out on a pilot plant scale is both time consuming and expensive. Thus, mathematical models can generate sets of data concerning the behaviour of the system quickly without incurring much cost, as compared to experimental study.

1.4 Objectives and Scope of Study

1.4.1 Objectives

The objectives of this study can be summarised as follows:

- a. To develop mathematical models for removal of high content CO₂ from CH₄ using membrane technology.
- b. To study and analyse the parameters that influence the permeability of CO₂ and CH₄, and separation behaviour of CO₂ removal system with high CO₂ concentration in the feed stream.

1.4.2 Scope of study

This study is divided into three phases. The first phase involves the development of a permeability model that could predict the mechanism of gas permeation in porous membrane as a function of pore size, operating pressure and temperature. After thorough understanding on the behaviour of gas permeation is obtained, the second phase will take place where it involves the development of a complete mixing model that could be useful to predict the separation factors of separation of CO₂ from CH₄ as a function of pore size, operating pressure, temperature, stage cut and the composition of CO₂ at the feed. The last phase of the study involves the investigation of the performance of this binary system by using a single – staged membrane separator, where necessary recommendations on the suitable operation would be identified and discussed.

CHAPTER 2

LITERATURE REVIEW

Transport phenomena in porous solids have been the subject of many studies. Quantitative solutions are obtained however only in a number of limiting cases of generally formulated problems or in relatively simple cases. Such a case is, e.g., the permeation of a single gas in a membrane system with relatively simple pore architecture and under conditions when a single mechanism is predominantly operating.

Transport of mixtures is more complicated, especially in membrane systems with a more complex architecture and operated with large pressure gradients. In such cases, quantitative solutions for permeation and separation efficiency (selectivity) are not available in a generally applicable form. Specific solutions have to be obtained by approximations and by combining solutions for limiting cases.

2.1 Important Concepts

Transport data of membrane can be expressed in terms of flux [$\text{mol.m}^{-2}.\text{s}^{-1}$] or as flux normalised per unit of pressure [$\text{mol.m}^{-2}.\text{s}^{-1}.\text{Pa}^{-1}$]. Following the IUPAC convention this last parameter is called permeation. Using 'permeation' is meaningful however only if there is a linear relation between flux and pressure. Despite the fact that this relation in many cases does not hold, transport data in the literature are expressed as permeation. To facilitate comparison of data, the permeation can be normalised per unit of thickness and is then called permeability [$\text{mol.m.m}^{-2}.\text{s}^{-1}.\text{Pa}^{-1}$]. This should be done only if the thickness of the separation layer is known. In many cases, only an unknown part of this layer is really active and use of the parameter permeability gives rise to large values compared with the real intrinsic ones. Therefore, in case of doubt, flux values should always be given together with the (partial) pressure of the

relevant components at the high-pressure (feed) and low-pressure (permeate) sides of the membrane, as well as the apparent membrane thickness.

An overview of various transport mechanisms in porous membranes is given in Table 2.1. The types of transport mechanisms are ranked accordingly to their significance in membrane gas separation based on researches by several expertises in this field.

Table 2.1: Transport regimes in porous membranes.

Transport Type	Pore range	References
Knudsen diffusion	2 – 50 nm	(1), (2), (3), (4)
Viscous flow (Molecular diffusion)	> 20 nm	(1), (2), (3), (4)
Surface diffusion	< 2 nm	(1), (2), (4)
Capillary condensation	< 2 nm (high pressure system)	(1), (3), (4)
Multilayer diffusion	< 2nm (high pressure system)	(1), (4)
Micropore diffusion	< 1.5 nm	(1)

(1) Burggraaf and Cot (1996)

(2) Cho *et al.*, (1995)

(3) Seader and Henley (1998)

(4) Hsieh (1996)

Viscous (Poiseuille) flow and molecular diffusion are non – selective. Nevertheless, they play an important role in the macroporous substrate(s) supporting the separation layer and can seriously affect the total flow resistance of the membrane system. Mesoporous separation layers or supports are frequently in the transient – regime between Knudsen diffusion and molecular diffusion, with large effects on the separation factor (selectivity). Surface diffusion will only occur at small pore regions, but it gives the highest selectivity due to membrane material's preferential sorptivity of certain gases than the others. Capillary condensation is reported to be obvious for system that involves CO₂ due to its plasticising effect on certain membrane material. Chapter 3 will elaborate more on the first four mechanisms due to their importance in membrane gas transport.

2.2 Pore Characteristics and Membrane Architecture

Porous materials have a very complex structure and morphology and many studies have been devoted to describing and characterising them. Roucquerol *et al.* (1994) in their IUPAC report give useful advice for terminology, definitions and characterisation strategies.

Parameters that influence transport properties in porous materials are porosity, pore size distribution, pore shape, interconnectivity and orientation. Indirectly particle size distribution and shape are important in the way they affect the uniformity of the pore size distribution, the pore shape and the roughness of the internal surface area.

Schematic diagram of different types of pores is given in Figure 2.1. As can be seen in the diagram, isolated pores and dead ends do not contribute to the permeation under steady conditions. Dead ends do also contribute to the porosity as measured by adsorption techniques but do not contribute to the effective porosity in permeation (Cunningham and Williams, 1980). Pore shapes are channel – like or slit – shaped. Pore constrictions are important for flow resistance, especially when capillary condensation and surface diffusion phenomena occur in systems with a relatively large internal surface area.

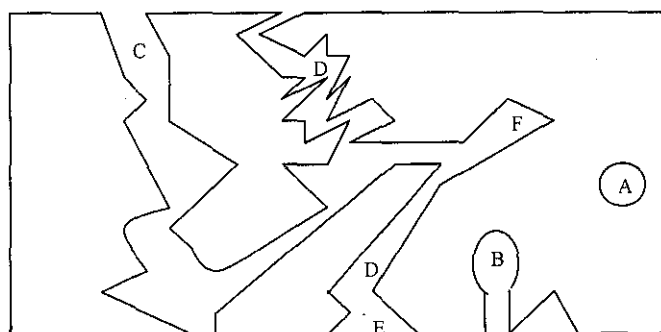


Figure 2.1: Schematic diagram of different types of pores in a porous solid. A: Isolated pore; B, F: dead end pores; C, D: Tortuous / rough pores; E: Conical pore.

2.3 Gas Permeability Model

Permeability is an important parameter in membrane characterisation. It gives an overview of permeation behaviour of a certain gas through a particular type of membrane, either highly permeable or less permeable. The measurement of gas permeability is normally done on pure gas specie. The following texts will illustrate and discuss some of the gas permeability models developed by several researchers.

The permeability, P'_i , for a pure gas i can be measured from the following equation (Seader and Henley, 1998):

$$P'_i = \frac{\varepsilon}{RT\tau} \left[\frac{1}{(1/D_i) + (1/D_{k,i})} \right] \quad (2.1)$$

Cho *et al.* (1995) developed an empirical model for gas permeability prediction based on the three most important transport mechanisms in membrane, namely viscous flow, Knudsen diffusion and surface diffusion. The model is shown as follows:

$$P'_i = \frac{\varepsilon\eta r_p^2}{8\mu_i RT} \bar{P} + \frac{2\varepsilon\eta r_p}{3RT} \left(\frac{8RT}{\pi M_i} \right)^{1/2} + \frac{2\varepsilon\eta D_s}{r_p AN_{av}} \frac{db_s}{dP} \quad (2.2)$$

The first term in the above equation represents the viscous flow. The second term caters for Knudsen diffusion whereas the third term describes the surface diffusion that occurs in the pores. It was noted in the original publication that the second term is not dimensional homogeneous with the first and third term. It should not contain the thickness of membrane in the equation. Equation 2.2 has been modified from this error as shown in the original publication so that it is dimensional homogeneous. The flaw in the relation as developed by Cho *et al.* (1995) is that when the pore size is so small that it approximates the size of a gas molecule, the effect due to pore refining is not obvious. Moreover, Knudsen diffusion will not occur when the pore size is smaller than the size of the gas molecule.

The value of gas permeability can also be determined experimentally as was done by Lee and Hwang (1985). It was shown that the gas permeability can be described by the following relation.

$$P'_i = \frac{q_p t_m}{A_m \Delta P} \quad (2.3)$$

From equation 2.3, it is obvious that permeability of gas through the membrane will increase with respect to increment in q_p , if the other parameters stay the same. This is true, as more gas permeates through the membrane surface. However, the permeability of gas should increase, by right, when the thickness of membrane decreases and not the other way around as suggested by equation 2.3. This is because the distant of travel of the gas molecules will decrease as the thickness reduces and thus the gas molecules need less time to complete the whole path. But, do not neglect the fact that the actual lengths of travel, t of the gas molecules are generally much longer than the membrane thickness, t_m , due to the intrinsic structure of the pores. As seen from equation 2.1, proposed by Seader and Henley (1998), permeability of gas is inversely proportional to the tortuosity of the membrane material, which is a ratio of t to t_m . Hence, it can be concluded that equation 2.3 is actually true, as the increase of t_m will result it a less tortuous membrane material and consequently shows an increase in permeability.

In the Dusty Gas Model (DGM) as presented by Mason and Malinaukas (1983), all the different contributions to the transport are taken into account. According to the model assumption, the wall of the porous medium is considered as a very heavy component and so contributes to the momentum transfer. The model is schematically represented in Figure 2.2 for a binary mixture. As can be seen from this electrical network analogy, the flux contributions by Knudsen diffusion $J_{k,i}$ and molecular diffusion of the mixture $J_{m,12}$ are in series and so are coupled. The total flux of component i ($i=1,2$) due to these contributions is $J_{i,km}$. The contribution of the viscous flow $J_{v,i}$ and of the surface diffusion $J_{s,i}$ are parallel with $J_{i,km}$ and so are considered independent of each other. There is no transport interaction between gas phase and surface diffusion.

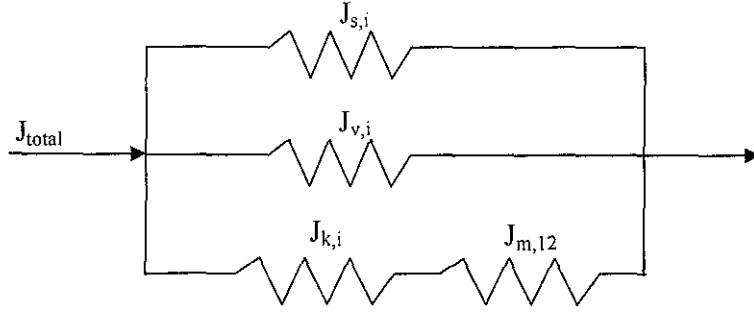


Figure 2.2: Schematic representation of Dusty Gas Model.

The flux expression for single specie i in a multi – component mixture with n components according to the DGM model results in (Burggraaf and Cot, 1996):

$$\sum_{j=1, j \neq i}^n \frac{x_i \cdot J_j - x_j \cdot J_i}{P_i D_{ij}^e} - \frac{J_i}{P D_{i,k}^e} = \frac{1}{RT} \frac{\delta x_i}{\delta z} + \frac{x_i}{PRT} \left(\frac{B_o P}{\eta D_{i,k}^e} + 1 \right) \frac{\delta P}{\delta z} \quad (2.4)$$

where, $D_{i,k}^e = \frac{\varepsilon^4}{\tau^3} K_n \sqrt{\frac{8RT}{\pi M_i}}$ with K_n as the Knudsen number and,

$$D_{ij}^e = 0.00262 \sqrt{\frac{T^3 \left[\frac{M_1 + M_2}{2M_1 M_2} \right]}{P \sigma_{12}^2 \Omega_{12}}}$$

Present and De Bethune (1949) were the first to develop a model (P – D model) including diffusion, intermolecular momentum transfer and viscous flow. Based on the P – D model, Eickmann and Werner (1985) incorporated two parameters (n_k and β) in the P – D equations to account for geometric and reflection characteristics of a real membrane. This extended P – D model is very successful to describe the effect of a variety of parameters on permeation and separation. Note that surface diffusion is not incorporated in the model. The flux of component i in a binary mixture is given by:

$$J_i = \frac{g'}{L} \left[\frac{\alpha_o}{1 + B' P} \frac{d(x.P)}{dz} + \frac{f_o B' x P}{1 + B' P} \frac{dP}{dz} + x A' P \frac{dP}{dz} \right] \quad (2.5)$$

with the mole fractions for components 1 and 2 ($i=1,2$) given by x and $1-x$, respectively. The first term in equation 2.5 describes the Knudsen diffusion, while the second and third term account for momentum transfer and viscous flow respectively. The different coefficients in equation 2.5 can be obtained from Burggraaf and Cot (1996).

2.4 Works on Flow Model by Others

In a membrane process, high – pressure feed gas is supplied to one side of the membrane and permeates normal to the membrane. The permeate leaves in a direction normal to the membrane, accumulating on the low – pressure side. Because of the very high diffusion coefficient in gases, concentration gradients in the gas phase in the direction normal to the surface of the membrane are quite small (Geankoplis, 1993). Hence, gas film resistances compared to the membrane resistance can be neglected. This means that the concentration in the gas phase in a direction perpendicular to the membrane is essentially uniform whether or not the gas stream is flowing parallel to the surface or not.

If the gas stream is flowing parallel to the membrane in essentially plug flow, a concentration gradient occurs in this direction. Hence, several cases can occur in the operation of a membrane module. The permeate side of the membrane can be operated so that the phase is completely mixed (uniform concentration) or where the phase is in plug flow. The high – pressure feed side can also be completely mixed or in plug flow. Counter – current or co – current feed side can also be used when both sides are in plug flow. Hence, separate theoretical models must be derived for these different types of operation.

In deriving theoretical models for gas separation by membranes, isothermal conditions and negligible pressure drop in the feed stream and permeate stream are generally assumed. It is also assumed that the effects of total pressure and / or composition of the gas are negligible and that the permeability of each component is constant (i.e., no interactions between different components). The important types of idealised flow patterns are summarised in Figure 2.3.

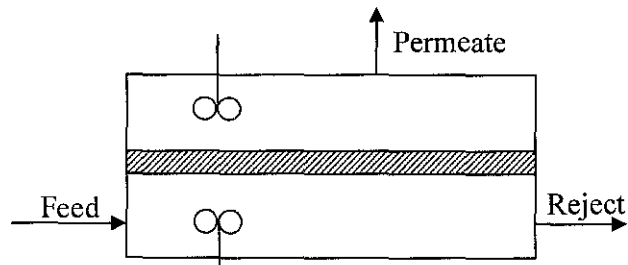


Figure 2.3a: Complete mixing model.

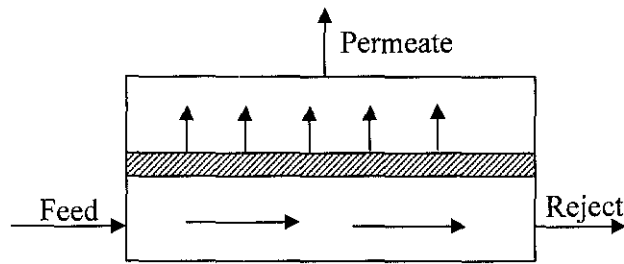


Figure 2.3b: Cross – flow model.

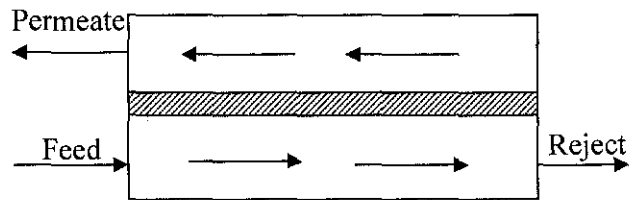


Figure 2.3c: Counter – current flow model.

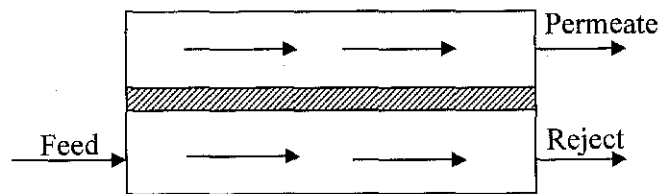


Figure 2.3d: Co – current flow model.

Weller and Steiner (1950) developed the complete mixing model and cross flow model for gas permeation. The former assumes complete mixing of the binary system either at the feed or permeate side whereas the latter assumes no mixing or interaction of the binary system in both the feed and permeate sides. Walawender and Stern (1972) then developed the complicated counter – current flow model while Blaisdell and Kammermeyer (1973) worked on the co – current flow model for gas permeation.

The models just described assume that the membrane module operated isothermally. However, the expansion of the residue (that is, high pressure) gas in a membrane module to the lower pressure in the permeate stream can be accompanied by a change in temperature if the gas mixture is non – ideal. The most common example of this effect is the well – known Joule – Thompson cooling of gas passing through an adiabatic expansion valve. In this process, gas enthalpy remains constant as the gas expands from high – pressure side of the valve to low – pressure side, but pressure and specific volume change. For non – ideal gases, this process can lead to the expanded gas being at either a higher or lower temperature than the compressed gas (Coker *et al.*, 1999).

Limited studies of the effects of expansion – driven cooling have been reported for membranes. Among the front – runners that accounts for temperature effects in their models are Rautenback and Dahm (1987), Gorissen (1987) and Cornelissen (1993).

Gorissen (1987) points out that large exit temperature changes were observed in CO₂ / CH₄ membrane – based separation. The exit temperature from the module was calculated to be 30°C lower than the feed temperature for a 40 mole% CO₂ mixture with CH₄ at a feed temperature of 40°C, a feed pressure of 70 bar, a permeate pressure of 2 bar, and a stage cut of 46%.

The recent work by Coker *et al.* (1999) explicitly accounts for heating or cooling inside membrane permeators due to gas expansion. It was cited that relative to an isothermal case, expansion – driven cooling reduces stage cut at a given feed flow rate since gas permeability decreases with decreasing temperature. It was highlighted that neglect of expansion – driven cooling in natural gas separation simulations can

lead to large errors in estimating the amount of feed gas that can be treated to achieve a fixed residue composition.

Despite the flaw of not accounting of non – isothermal effect in the operation, the idealised complete mixing model will be the main interest of this research as a starting point for membrane separation modelling because it is more practical and true to determine the mole composition at the permeate side. This model will be further elaborated in the following chapter.

CHAPTER 3

THEORY

3.1 Gas Transport in Porous Material

The properties of gas flow in porous media depend on the ratio of the number of molecule – molecule collisions to that of the molecule – wall collisions. The Knudsen number Kn is a characteristic parameter defining different regions of this ratio.

As mentioned in chapter 2, there are four types of flows that predominate the transport of gas molecules in the pores, namely viscous diffusion, Knudsen diffusion, surface diffusion and capillary condensation. Figure 3.1 shows the schematic drawings of these flows.

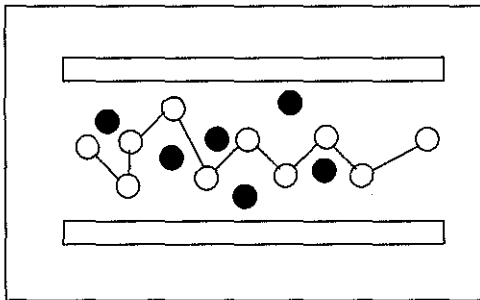


Figure 3.1a: Viscous diffusion.

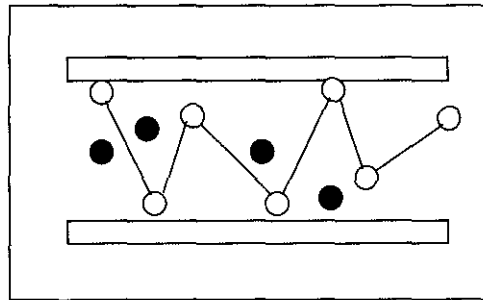


Figure 3.1b: Knudsen diffusion.

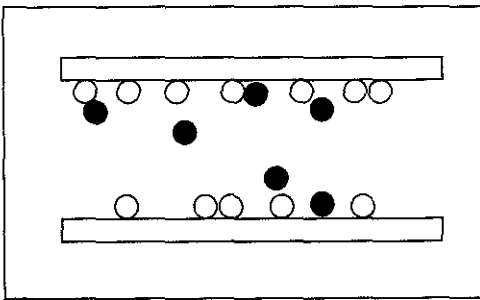


Figure 3.1c: Surface diffusion.

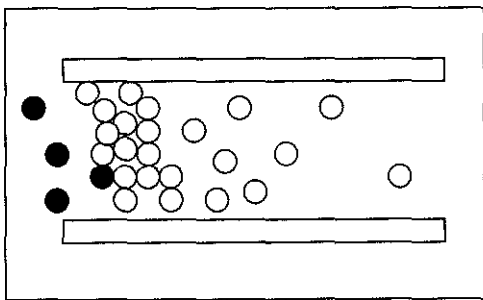


Figure 3.1d: Capillary condensation.

3.1.1 Viscous Diffusion

The assumption that the pore resembles a perfect cylinder is necessary to model the viscous flow in the pore (Bird *et al.*, 1960). This assumption is practical for a piece of thin membrane with pore size ranging from 1 – 7 nm, as the gas molecules will collide against each other more frequently than their collision with the cylinder wall, under this condition. The average velocity of gas molecule has been published by Bird *et al.* (1960) as follow:

$$v_{av} = \frac{1}{2} \left[\frac{p_h - p_l}{4\mu_l t} \right] r_p^2 \quad (3.1)$$

From equation 3.1, the volumetric flow rate of the gas across the pores can be computed by simply multiplying v_{av} with the cross sectional area of the pores. For total volumetric flow rate across the whole piece of membrane, the number of pores q_p need to be calculated in prior, as such:

$$\begin{aligned} \# \text{ of Pore} &= \varepsilon \left(\frac{\text{Membrane area}}{\text{Cross sectional area of pore}} \right) \\ &= \varepsilon \left(\frac{2\pi R_m L_m}{\pi r_p^2} \right) \\ &= \frac{2\varepsilon R_m L_m}{r_p^2} \end{aligned} \quad (3.2)$$

$$\begin{aligned} q_p &= \left(v_{av} \pi r_p^2 \right) \left(\frac{2\varepsilon R_m L_m}{r_p^2} \right) \\ &= \frac{1}{2} \left(\frac{p_h - p_l}{4\mu_l t} \right) r_p^2 \pi r_p^2 \left(\frac{2\varepsilon R_m L_m}{r_p^2} \right) \\ &= \frac{\varepsilon \pi R_m L_m r_p^2}{4\mu_l t} (p_h - p_l) \end{aligned} \quad (3.3)$$

From equation 2.3 and 3.3, the permeability of gas molecule through the membrane pores, due to viscous diffusion, can thus be computed as such:

$$\begin{aligned}
 P_i &= \frac{q_p t_m}{A_m \Delta P} \\
 &= \frac{\varepsilon \pi R_m L_m r_p^2 (p_h - p_l) t_m}{4 \mu_i t (2 \pi R_m L_m) (p_h - p_l)} \\
 &= \frac{\varepsilon r_p^2 t_m}{8 \mu_i t} \\
 &= \frac{\varepsilon r_p^2}{8 \tau \mu_i}
 \end{aligned} \tag{3.4}$$

Equation 3.4 shows that the permeability of gas molecule does not depend on the pressure of the system. It is only a function of the membrane porosity, pore size, tortuosity and the viscosity of gas. It is important to note that the permeability of gas is a function of temperature indirectly, as the viscosity of gas varies with system temperature. The viscosity of gas can be computed by using the empirical correlation as established by Bird *et al.* (1960):

$$\mu_i = 2.6693 \times 10^{-5} \frac{\sqrt{M_i T}}{\sigma^2 \Omega_\mu} \tag{3.5}$$

3.1.2 Gas Diffusion

The flaw in using equation 3.4 to predict the permeability of gas is that it is very much limited to the condition when the mean free path of travel of the gas molecule is smaller than the pore diameter (viscous mechanism) (Othman, 2001). Under this condition, the collision between gas molecules is more often than the collision of gas molecule against the pore wall, as shown in Figure 3.1a. However, when the system temperature is held high and the pressure is held low, the mean free path of travel of the gas molecule became larger and the collision between gas molecules against the pore wall predominates. Thus, Knudsen diffusion and ordinary diffusion occurs (Seader and Henley, 1998) via the following relation:

$$D_g = \varepsilon \left(\frac{1}{1/D_i + 1/D_{k,i}} \right) \quad (3.6)$$

Following the above correlation, the flux of gas, J_g , as a result of gas diffusion can be written as:

$$J_g = -D_g \frac{dC_g}{dZ} \quad (3.7)$$

By inserting D_g from (3.6) into equation (3.7) and substituting $C_g = \frac{P}{zRT}$ from ideal gas law yields:

$$J_g = -\frac{\varepsilon}{zRT} \left(\frac{1}{1/D_i + 1/D_{k,i}} \right) \frac{dP}{dZ} \quad (3.8)$$

Stastna and De Kee (1995) defined the ordinary gas diffusion, D_i as:

$$\frac{\bar{P} D_{AB}}{(P_{cA} P_{cB})^{1/3} (T_{cA} T_{cB})^{5/12} \left(\frac{1}{M_A} + \frac{1}{M_B} \right)^{1/2}} = a \left(\frac{T}{\sqrt{T_{cA} T_{cB}}} \right)^b \quad (3.9)$$

where $a = 2.745 \times 10^{-4}$ and $b = 1.823$, as obtained from Stastna and De Kee (1995). In calculating the ordinary gas diffusion by using equation 3.9, it is important to note that gas specie A is assumed to diffuse through the pores via the other gas species that stay in stagnant condition (Treybal, 1981).

Knudsen diffusion predominates when the frequency of collision between the gas molecules and pore walls increases. Atkins (1994) showed the correlation for Knudsen diffusion as below:

$$D_{k,i} = \frac{1}{3} \lambda \bar{c} \quad (3.10)$$

Further derivation from Maxwell expression relates \bar{c} as below (Atkins, 1994):

$$\bar{c} = \sqrt{\frac{8RT}{\pi M_i}} \quad (3.11)$$

Upon the occurrence of Knudsen diffusion, the mean free path of gas molecule is greater or equal to the diameter of the pore, that is $2r_p$. The effective mean free path of travel of the gas molecule can thus be obtained by deducting the diameter of gas molecule from the pore diameter, as shown in Figure 3.2.

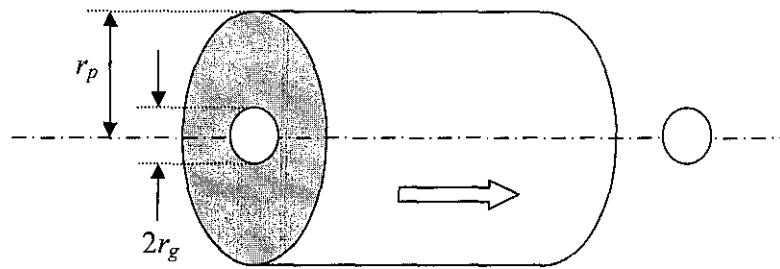


Figure 3.2: Cross sectional view of collision in the pore.

When λ is replaced with the effective mean free path of travel that is equivalence to $2(r_p - r_g)$, rearrangement of equation 3.10 yields the correlation for Knudsen diffusion that accounts for effective mean free path of travel of the gas molecules.

$$D_{k,i} = \frac{2(r_p - r_{g,i})}{3} \sqrt{\frac{8RT}{\pi M_i}} \quad (3.12)$$

It is important to note that Knudsen diffusion is valid in the case of $r_p \geq r_{g,i}$. In the occasion where the pore size is smaller than the size of the gas molecules, there will not be any diffusion of gas molecules through the pores of the membrane.

3.1.3 Surface Diffusion

When the temperature of the gas is such that adsorption on pore walls is important, experimental results show that the preceding laws for gaseous flow are no longer valid (Burggraaf and Cot, 1996). For relatively low surface concentrations, the surface flux, J_s , for a single gas is generally described by the two-dimensional Fick's law (Burggraaf and Cot, 1996):

$$J_s = -2 \frac{t_m \varepsilon^2}{r_p \tau} (1 - \varepsilon) D_s \frac{dC_s}{dZ} \quad (3.13)$$

The surface concentration, C_s , can be correlated with the membrane density, ρ_m , and the uptake of the gas molecules by the sorbent material, h , which has the unit of [mol.g⁻¹] by the following equation (Othman, 2001):

$$C_s = \rho_m h \quad (3.14)$$

By inserting equation 3.14 into equation 3.13 yields:

$$\begin{aligned} J_s &= -2 \frac{t_m \varepsilon^2}{r_p \tau} (1 - \varepsilon) D_s \frac{d(\rho_m h)}{dZ} \\ &= -2 \frac{t_m \varepsilon^2}{r_p \tau} (1 - \varepsilon) D_s \rho_m \frac{dh}{dZ} \end{aligned} \quad (3.15)$$

The uptake of the gas specie by the sorbent material, h , is approximated by Henry's law (monolayer adsorption is assumed to take place) to be directly proportional to the equilibrium loading factor, f , and system pressure as below:

$$h \propto fP \quad (3.16)$$

Dimensional analysis of equation 3.16 yields:

$$h = \frac{1}{zRT} (fP) \quad (3.17)$$

Keizer *et al.* (1988) showed that f is directly proportional to pressure and inversely proportional to temperature. By inserting h from equation 3.17 into equation 3.15 yields:

$$\begin{aligned} J_s &= -2 \frac{r_p \varepsilon^2}{t_m \tau} (1 - \varepsilon) D_s \rho_m \frac{d(fP)}{zRT dZ} \\ &= -2 \frac{r_p \varepsilon^2}{t_m \tau} (1 - \varepsilon) \frac{D_s \rho_m f}{zRT} \frac{dP}{dZ} \end{aligned} \quad (3.18)$$

where D_s can be computed from the following empirical relation as established by Bird *et al.* (1960):

$$D_s = 1.6 \times 10^{-2} e^{\left[-0.45 \frac{(-\Delta H_{ads})}{mRT} \right]} \quad (3.19)$$

where m is 2 for conductive sorbent and 1 for non-conductive sorbent. Heat of adsorption of the gas specie to the sorbent material can be approximated with the assumption that condensation occurs on the surface. It can be estimated by using Trouton's law and Watson Correlation (Felder and Rousseau, 1986).

With gas mixtures, enhancement of the separation factor can be obtained by preferential sorption of mobile species of one of the components of the gas mixture. Adsorption does not always lead to enhanced separation. In a mixture of light non-adsorbing molecules and heavy molecules, the heavy molecules move slower than the lighter ones but in many cases are preferentially adsorbed. Consequently, the flux of the heavier molecules is better enhanced by surface diffusion and the separation factor increases. This occurs, e.g., in $\text{CH}_4 / \text{CO}_2$ mixtures in Vycor glass membrane (Burggraaf and Cot, 1996). With two adsorbing molecular species, competition for the adsorption sites may exist and sorption isotherms for single gas species are no longer valid (Uhlhorn *et al.*, 1989).

Pore distribution of the membrane material is normally not uniform and the pores can have very different shape, orientation and length from each other. Thus, the diffusion of gas molecules through all the pores in a membrane system may not be necessary uniform or successful. Effective diffusion, D_e is introduced to cater for this discrepancy between pores, and it can be obtained from Fick's Law as,

$$J_T = -D_e \frac{dC}{dZ} \quad (3.20)$$

J_T is the total flux that comprises the flux via gas diffusion and surface diffusion.

Substitution of $C = \frac{P}{zRT}$ into equation 3.20 yields,

$$J_T = -\frac{D_e}{zRT} \frac{dP}{dZ} \quad (3.21)$$

From the true definition of J_T , the total flux can be written as,

$$\begin{aligned} J_T &= J_g + J_s \\ &= -\frac{\varepsilon}{zRT} \left(\frac{1}{1/D_i + 1/D_{k,i}} \right) \frac{dP}{dZ} - 2 \frac{t_m \varepsilon^2}{r_p \tau} (1 - \varepsilon) \frac{D_s \rho_m f}{zRT} \frac{dP}{dZ} \end{aligned} \quad (3.22)$$

By equating equation 3.22 to equation 3.20, D_e is obtained as such,

$$D_e = \varepsilon \left(\frac{1}{1/D_i + 1/D_{k,i}} \right) + 2 \frac{t_m \varepsilon^2}{r_p \tau} (1 - \varepsilon) D_s \rho_m f \quad (3.23)$$

3.1.4 Capillary Condensation

With increasing pressure and at temperatures below the critical temperature, the surface coverage (occupancy) can become larger than unity. In this case the adsorbed molecules behave like a sliding film on the internal surface of the porous membrane under the action of a bi – dimensional spreading pressure related to the gas pressure.

Capillary condensation is said to occur when, in porous solids, multilayer adsorption from vapour proceeds to the point at which pores are filled with liquid separated from the gas phase by menisci. The concept of capillary condensation loses its sense when the dimensions of the pores are so small that the term meniscus ceases to have a physical significance. Capillary condensation is most often accompanied by hysteresis (Burggraaf and Cot, 1996). It is important to note that the model for capillary condensation will not be included in this modelling work, as it is assumed that multilayer adsorption does not take place at small pores in the membrane.

3.2 Gas Permeability as An Integration of All Transport Mechanism

Permeability of gas molecule in porous material has combined influences by all the three types of transport mechanism, as discussed earlier in Section 3.1.1 to 3.1.3. The trans – membrane flux of a gas specie, N , can be related as follow,

$$N = \frac{P'_i}{t_m} (p_h - p_l) \quad (3.24)$$

By equating equation 3.24 with equation 3.22, which is $N = J_T$,

$$\begin{aligned} \frac{P'_i}{t_m} (p_h - p_l) &= \frac{D_e}{z\tau RT} (p_h - p_l) \\ \therefore P'_i &= \frac{D_e}{z\tau RT} (p_h - p_l) \frac{t_m}{(p_h - p_l)} \end{aligned} \quad (3.25)$$

Knowing that $\tau = \frac{t}{t_m}$, hence,

$$\therefore P'_i = \frac{D_e}{z\tau RT} \quad (3.26)$$

By substituting the relation for D_e from equation 3.23 into the above equation,

$$\begin{aligned}
P'_i &= \frac{\varepsilon \left(\frac{1}{1/D_i + 1/D_{k,i}} \right) + 2 \frac{t_m \varepsilon^2}{r_p \tau} (1 - \varepsilon) D_s \rho_m f}{z \tau RT} \\
&= \frac{\varepsilon}{z \tau RT} \left(\frac{1}{1/D_i + 1/D_{k,i}} + 2 \frac{t_m \varepsilon}{r_p \tau} (1 - \varepsilon) D_s \rho_m f \right)
\end{aligned} \tag{3.27}$$

Permeability of gas as the result of viscous diffusion, as shown in equation 3.4 can be unified with equation 3.27 to model the characteristic model of gas permeability as a function of the three important mechanisms of transport in pores,

$$P'_i = \frac{\varepsilon r_p^2}{8 \tau \mu_i} + \frac{\varepsilon}{z \tau RT} \left[\left(\frac{1}{1/D_i + 1/D_{k,i}} \right) + 2 \frac{t_m \varepsilon}{r_p \tau} (1 - \varepsilon) (D_s \rho_m f) \right] \tag{3.28}$$

Dimensional analysis of the above equation shows that term 1 [$\text{m}^3 \cdot \text{s} \cdot \text{kg}^{-1}$] is not dimensional homogeneous with term 2 and 3 [$\text{mol} \cdot \text{s} \cdot \text{kg}^{-1}$]. Introduction of ideal gas law into term 1 will yield a dimensional homogeneous equation for gas permeability. From ideal gas law,

$$\begin{aligned}
PV &= znRT \\
\frac{n}{V} &= \frac{P}{zRT}
\end{aligned} \tag{3.29}$$

Substitution of equation 3.29 into equation 3.28,

$$\begin{aligned}
P'_i &= \frac{\varepsilon r_p^2 P}{8 \tau \mu_i z RT} + \frac{\varepsilon}{z \tau RT} \left[\left(\frac{1}{1/D_i + 1/D_{k,i}} \right) + 2 \frac{t_m \varepsilon}{r_p \tau} (1 - \varepsilon) (D_s \rho_m f) \right] \\
&= \frac{\varepsilon}{z \tau RT} \left[\frac{r_p^2 P}{8 \mu_i} + \left[\left(\frac{1}{1/D_i + 1/D_{k,i}} \right) + 2 \frac{t_m \varepsilon}{r_p \tau} (1 - \varepsilon) (D_s \rho_m f) \right] \right]
\end{aligned} \tag{3.30}$$

It is important to note that the pressure as mentioned in equation 3.30 is the pressure in the membrane pores. However, the measurement of pressure in the pores will be cumbersome and impractical. Thus, the pressure in the pores can be approximated as the average pressure between the feed and permeate side (Othman, 2001).

The contribution of viscous flow towards the permeability of gas is directly proportional to the average pressure between feed and permeate side. It may lose its entire effect towards permeability at high temperature, as the gas viscosity is a strong function of temperature. However, for small and fine pores, the contribution of surface diffusion is more apparent.

3.3 Permeability of Gas in Mixture

For calculation of gas permeability in a mixture, the average viscosity and ordinary diffusion need to be taken into account to cater for the interaction between different gas species. For gas in a binary mixture, the permeability can be computed via the following equation.

$$P_{i,mix}^v = \frac{\varepsilon}{z\tau RT} \left[\frac{r_p^2 P}{8\mu_{mix}} + \left[\left(\frac{1}{1/D_{i,mix} + 1/D_{k,i}} \right) + 2 \frac{t_m \varepsilon}{r_p \tau} (1 - \varepsilon) (D_s \rho_m f) \right] \right] \quad (3.31)$$

For gases in a mixture, the average viscosity of the gas mixture can be calculated from the following equation (Bird *et al.*, 1960).

$$\mu_{i,mix} = \frac{\sum_{i=1}^n x_i \mu_i}{\sum_{j=1}^n x_j \Phi_{i,j}} \quad (3.32)$$

where x_i is the mole fraction of gas specie i in the mixture. $\Phi_{i,j}$ is a constant and can be computed with the following empirical correlation as in equation 3.33 (Bird *et al.*, 1960).

$$\Phi_{i,j} = \frac{1}{\sqrt{8}} \left(1 + \frac{M_j}{M_i} \right)^{-\frac{1}{2}} \left[1 + \left(\frac{\mu_i}{\mu_j} \right)^{\frac{1}{2}} \left(\frac{M_j}{M_i} \right)^{\frac{1}{4}} \right]^2 \quad (3.33)$$

For gas ordinary diffusion in a mixture, it can be computed taking into account the effect of mole fraction of other gas species as such (Treybal, 1981),

$$D_{i,mix} = \frac{1}{\frac{x_j}{D_{i,j}} + \frac{x_k}{D_{i,k}} + \dots + \frac{x_n}{D_{i,n}}} \quad (3.34)$$

3.4 Separation Factor

The parameter to describe the separation efficiency for a binary mixture is the separation factor α , which is a measure of the enrichment of a gas component after it has passed the membrane. Vieth (1991) suggests that the ideal separation factor for a binary system can be written as,

$$\alpha^* = \frac{P'_A}{P'_B} \quad (3.35)$$

For a given mixture, α^* is influenced by the membrane and the process specific parameters as discussed earlier. In mesopore, the most effective separation mechanism outside the capillary condensation region is Knudsen diffusion. In this case the ideal separation factor α^* equals the square root of the ratio of molecular weights:

$$\alpha^* = \sqrt{\frac{M_B}{M_A}} \text{ with } M_B > M_A \quad (3.36)$$

In actual, α^* is not equal to α due to back diffusion, caused by non – zero pressure at the permeate side, or the contributions of non – separative mechanism to the total flow and concentration polarisation on feed or the permeate side. Also, the presence of surface diffusion influences the ideal separation factor.

Back diffusion that is due to a non – zero value of pressure at the permeate side is a very general phenomenon to decrease the value of α . The permeate gases at the

permeate side of the membrane are removed by compressing or by a sweep gas. If the pressure at the downstream (permeate) side is in the transition or continuum regime and is not negligible, there is a back – diffusion flux into the membrane. Equation 3.37 gives the effect of back diffusion on the actual separation factor (Burggraaf and Cot, 1996).

$$\alpha = 1 + \frac{(1 - P_r)(\alpha^* - 1)}{1 + P_r(1 - \gamma)(\alpha^* - 1)} \quad (3.37)$$

It is obvious from equation 3.37 that the permeate pressure directly after the separation layer should be kept low to yield a more attractive and enhanced separation factor for the binary mixture.

3.5 Complete Mixing Model

Figure 3.3 is a detailed process flow diagram for complete mixing model. When a separator element is operated at a low recovery (i.e., where the permeate flow rate is a small fraction of the entering feed rate), there is a minimal change in composition. Then the results derived using the complete – mixing model provide reasonable estimates of the permeate purity. This case is developed by Weller and Steiner (1950).

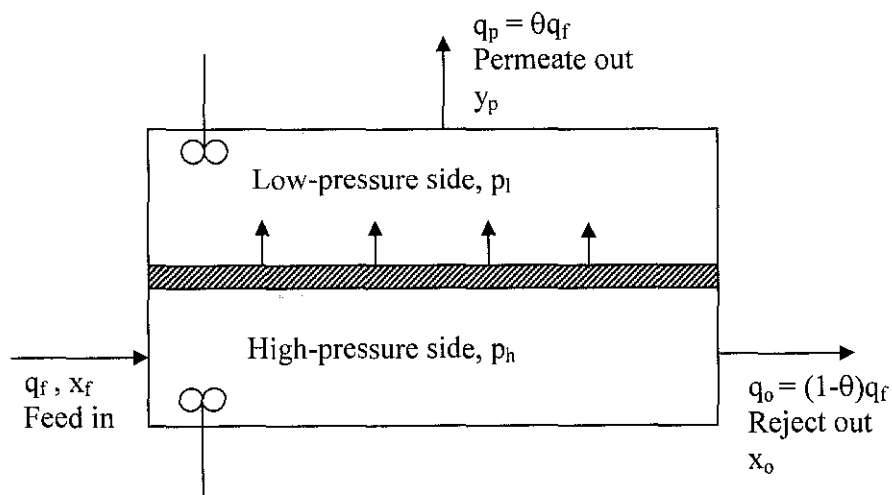


Figure 3.3: Detailed process flow for complete mixing model.

The overall material balance (Figure 3.3) is as follows:

$$q_f = q_o + q_p \quad (3.38)$$

The cut or fraction of feed permeated, θ , is given as,

$$\theta = \frac{q_p}{q_f} \quad (3.39)$$

The rate of diffusion or permeation of species A (in a binary of A and B) is given as,

$$\frac{q_A}{A_m} = \frac{q_p y_p}{A_m} = \left(\frac{P'_A}{t_m} \right) (p_h x_o - p_l y_p) \quad (3.40)$$

A similar equation can be written for component B,

$$\frac{q_B}{A_m} = \frac{q_p (1 - y_p)}{A_m} = \left(\frac{P'_B}{t_m} \right) (p_h (1 - x_o) - p_l (1 - y_p)) \quad (3.41)$$

Dividing equation 3.40 by equation 3.41,

$$\frac{y_p}{1 - y_p} = \frac{\alpha^* [x_o - (p_l / p_h) y_p]}{(1 - x_o) - (p_l / p_h) (1 - y_p)} \quad (3.42)$$

Making an overall material balance on component A,

$$q_f x_f = q_o x_o + q_p y_p \quad (3.43)$$

Dividing by q_f and solving for the outlet reject composition,

$$x_o = \frac{x_f - \theta y_p}{1 - \theta} \quad (3.44)$$

CHAPTER 4

METHODOLOGY

4.1 Model Development

4.1.1 Assumptions in Model Development

Assumptions are important in order for the models developed to be meaningful. Below are the few assumptions made in this modelling work:

1. The membrane is assumed to be operated isothermally with negligible pressure drop in the feed and retentate side. The effect of Joule – Thompson expansion of gas will not be considered in this study.
2. Complete mixing occurs in both the feed and permeate chamber and that the bulk gas phase is moving in a plug flow manner.
3. No reaction occurs in the membrane separator.
4. Monolayer adsorption is assumed to take place in the membrane material. Capillary condensation (multilayer adsorption) is possible in the membrane material but is assumed not to take place in this study. This is due to the monolayer adsorption assumption in surface diffusion.

4.1.2 Basic Equations Used

The study of gas permeability of pure CO₂ and CH₄ is done based on equation 3.30, as developed. On the other hand, the study of gas permeability of CO₂ and CH₄ in CO₂ / CH₄ mixture is done based on equation 3.31. For study of separation behaviour of this binary mixture, results simulated based on equation 3.30 and 3.31 as a function of various process parameters, is studied by using equation 3.37, which accounts for back pressure effect in the permeate side. There are many more

supporting equations used to supplement the use of equation 3.30, 3.31 and 3.37 mentioned, as can be seen in Figure 4.1 and 4.2 respectively.

4.1.3 Features of the Models

There are 2 new improvements made in this modelling work that differentiate it from other works such as the one by Cho *et al.*, (1995), Dusty Gas Model and extended P – D model as cited in Chapter 2. First, the effect of pore refining in the Knudsen diffusivity is taken into account in this modelling work. This is because Knudsen diffusion occurs based on the mean free path available in the pores. Equation 3.12 shows that Knudsen diffusivity term will become negative if the pore size is less than the radius of the gas molecules. Negative diffusivity simply means no diffusion is encountered under such condition. As mentioned in Chapter 2, model by Cho *et al.* (1995) does not take this factor into account. Secondly, Henry's law adsorption behaviour is incorporated into the surface diffusivity term, as shown in equations 3.16 to 3.18. Although Henry's law might not be accurate to predict the adsorption behaviour of the gas molecules, this modelling serves as the platform that incorporates any of the adsorption isotherms into the surface diffusivity term, by inserting the most simple adsorption isotherm into the model.

4.2 Software Required

Mathcad 11.0 Enterprise version is required to perform sensitivity analysis on the models developed. Mathcad is a software program that uses a unique method to manipulate formulas, numbers, text, and graphs. Unlike programming languages, the equations are written as they would appear in a mathematics reference book, against a background screen in which descriptive text may be placed arbitrarily. The equations may be solved analytically or numerically. The combination of equations, text, and diagrams in an open – screen environment makes application development easy.

Microsoft Excel will supplement the extension work to analyse the data generated by Mathcad simulation. Trending of results will be done using this powerful tool. The ease of use and its variety of function tools make Microsoft Excel favourable in this project when dealing with multiple lines on a same graphical representation.

4.3 Membrane Properties

γ -alumina and acetate cellulose are two types of membrane chosen to assist this modelling work. The former is an inorganic membrane whereas the latter is an organic membrane. Experimental data obtained for the latter will be fitted into the simulation results to study the validity and reliability of the model. Table 4.1 shows the properties of these membrane materials.

Table 4.1: Properties of γ -alumina and acetate cellulose membrane.

Properties	γ -alumina*	acetate cellulose**
Pore size range, nm	0.15 – 290.00	0.60 – 3.70
$t_m, \mu m$	0.10	0.60
ϵ	0.603	0.722
τ	1.658	1.390

* Data adopted from Keizer *et al.*(1988)

** Data adopted from Matsuura (1993)

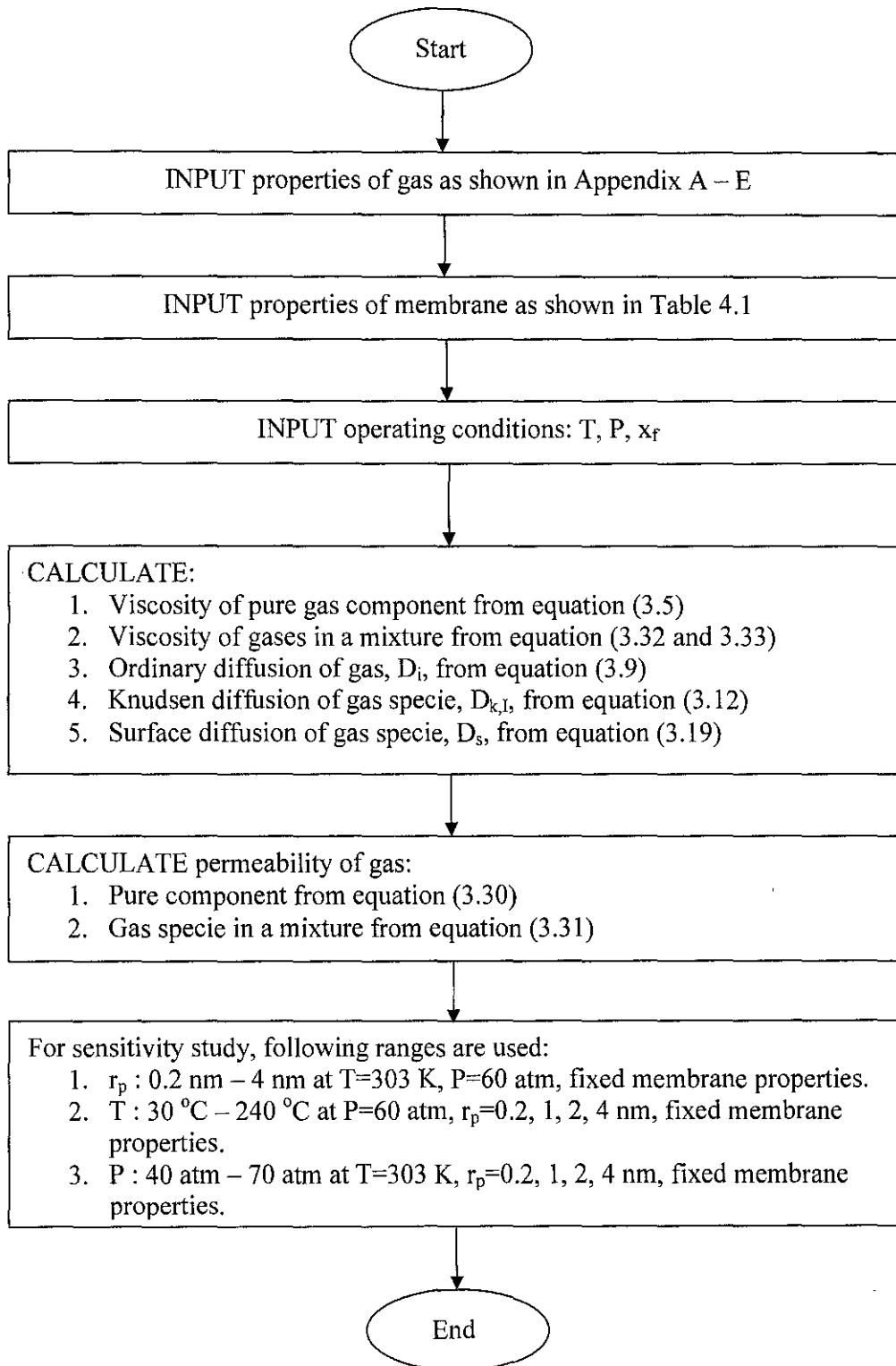


Figure 4.1: Algorithm to solve the model for both pure gas permeability and permeability of gas specie in a mixture.

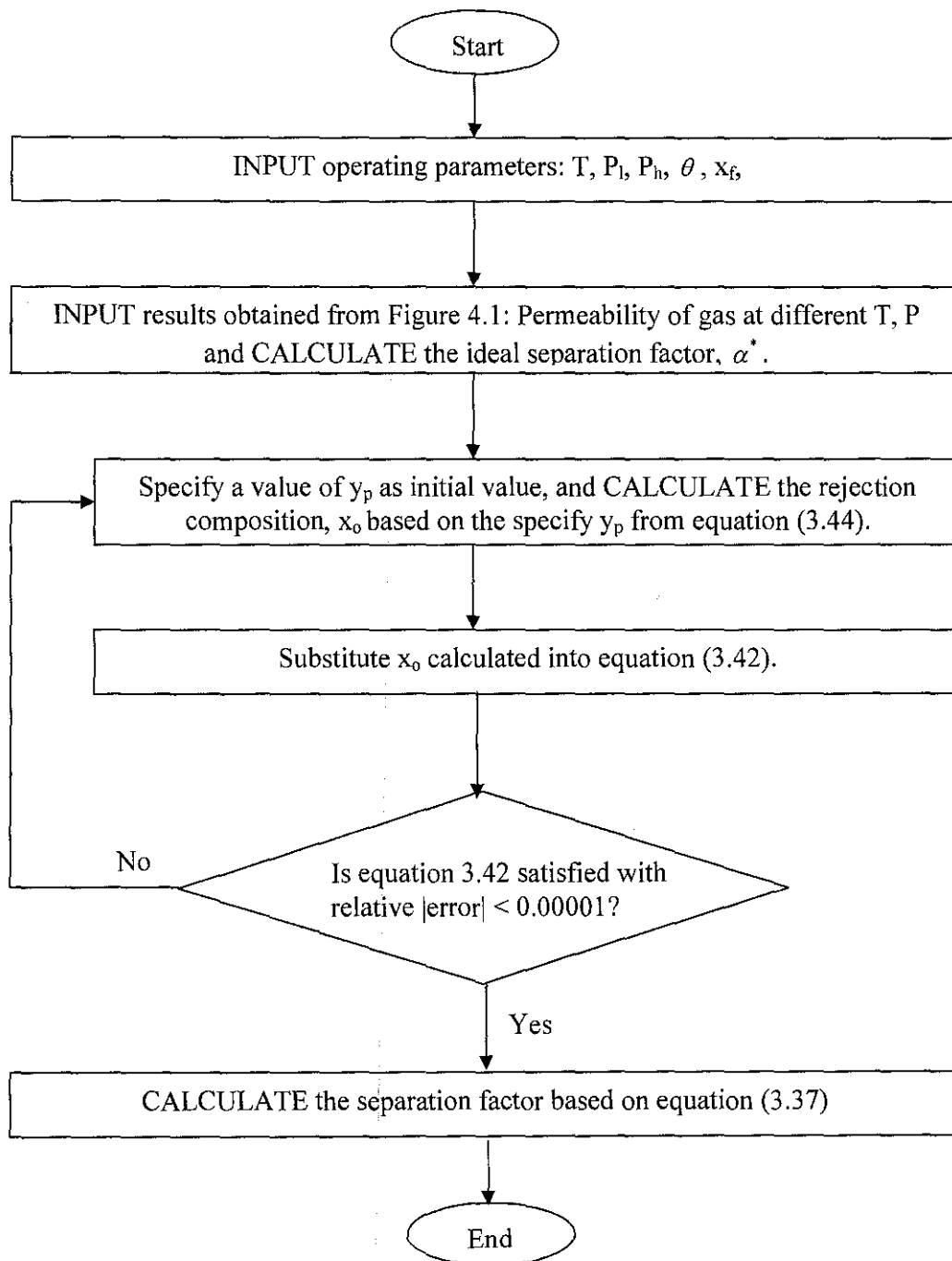


Figure 4.2: Algorithm to solve the model to compute the separation factor for CO₂ / CH₄ separation.

CHAPTER 5

RESULTS AND DISCUSSION

The study of membrane separation of binary gases system requires good understanding of the individual gas permeability through the porous material. The first half of this chapter would cover the study of gas permeability in porous membrane due to different operating conditions while the second half of the chapter would report on the separation behaviour of CO₂ / CH₄ binary system. All simulation results are based on the details supplied in Chapter 4.

5.1 Mechanisms of Flow of Gas Molecules in Porous Membrane

As mentioned in Chapter 2 and 3, the dominant mechanisms of gas permeation in porous material consist of (1) viscous diffusion, (2) Knudsen diffusion and (3) surface diffusion. Along the simulation of the models, it was assumed that the surface diffusion, which comprises the adsorption of gas molecules onto the surface of the pores and then glide along the pores upon the pressure gradient, would behave as ideally as predicted by Henry's law. Another phenomenon on surface science, which is the capillary condensation, was not considered due to the monolayer adsorption assumption made earlier (Refer Section 4.1.1). As obtained from Burggraaf and Cot (1996), capillary condensation (multiplayer diffusion) would take place at high pressures and temperatures well below the critical temperature of the adsorbed molecule, which is deemed not applicable in this study.

5.1.1 Effect of Pore Size on Gas Permeability

A study was carried out to observe the trends of gas permeation in porous membrane in the pore size range of 0.2 nm – 2 nm, which is the normal range for gas separation

(Uhlhorn and Burggraaf, 1990). As can be seen from Figure 5.1, surface diffusion is the dominant contributor to total permeability of CO₂ at small pores and it decreases with increasing pore size. This is in accordance to the theory as suggested by Hsieh (1996). At small pore sizes, the movement of the gas molecules are impeded by the narrow pathways of travel. Under this condition, the gas molecules have higher tendency to diffuse from the bulk stagnant gas film to the pore surface due to the concentration gradient between bulk gas phase and pore surface. At the pore surface, adsorption of CO₂ gas molecules (strongly adsorbing gas) takes place and thus contribute to the high total permeability of CO₂. Due to the hindered pathways of travel, viscous diffusion and Knudsen diffusion are not apparent at small pore sizes.

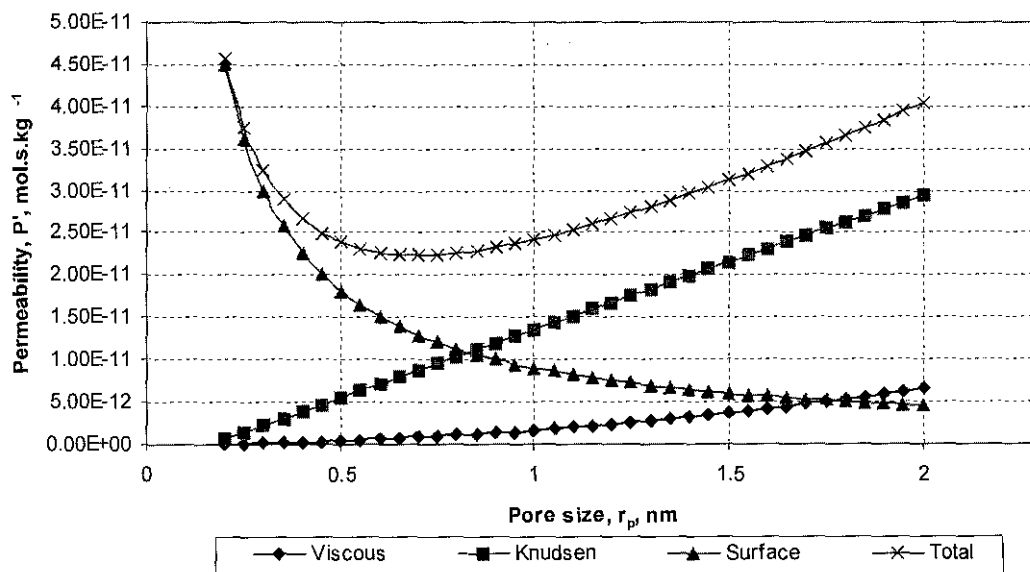


Figure 5.1: Effect of pore size on the mechanisms of flow for pure CO₂ in γ -alumina membrane at T=303 K, P=60 atm.

At higher pore size, Knudsen diffusion becomes more apparent and contributes the most to total permeability of pure CO₂ molecules across the alumina membrane. This is because higher pore size would provide more mean free pathways for the transport of gas molecules. The CO₂ molecules would now collide more frequently with the pore walls rather than colliding with the neighbouring CO₂ molecules (viscous diffusion). This is again in accordance with the theory as obtained from Burggraaf and Cot (1996) as well as modelling work by Othman (2001).

As for CH₄ molecules, same trend was observed. As compared to CO₂, CH₄ has much lower adsorptivity and thus the effect of surface diffusion is not that dominant at small pore sizes. Hsieh (1996) reports that the ratio of CO₂ adsorptivity to CH₄ adsorptivity on alumina membrane is approximately 20. As from Figure 5.2, Knudsen diffusion for CH₄ molecules becomes more dominant at pore sizes beyond 0.5 nm. While surface diffusion continues to lose its effect on total permeability of CH₄ with increasing pore size, viscous diffusion becomes relatively important after Knudsen diffusion towards the transport of CH₄ molecules across the membrane.

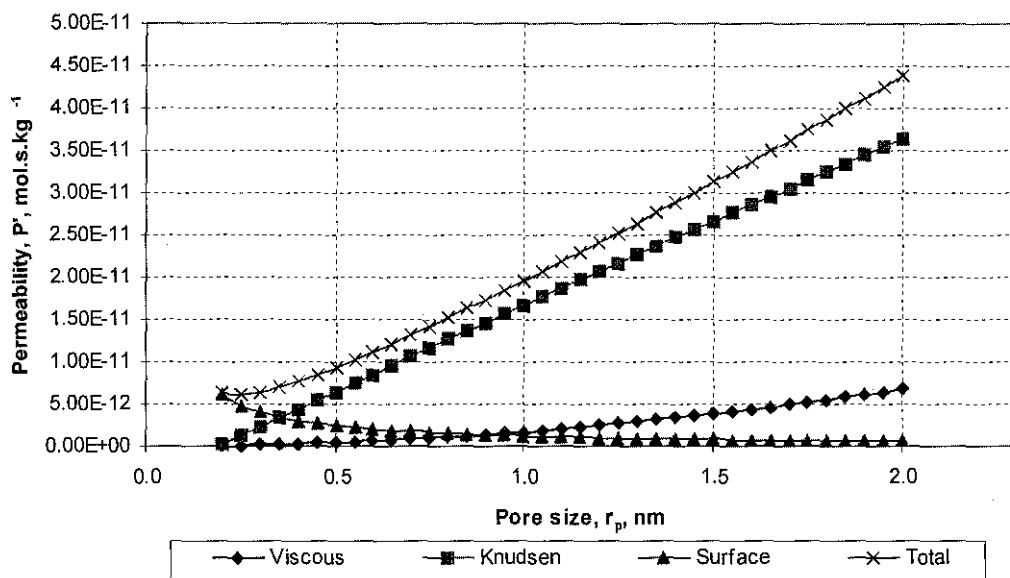


Figure 5.2: Effect of pore size on the mechanisms of flow for pure CH₄ in γ -alumina membrane at T=303 K, P=60 atm.

Generally, increasing pore size of the membrane material would improve the transport of gas molecules in the porous material due to larger mean free pathways for the gas molecules to diffuse through. However, this increment in pore size would result in unnecessary sacrifice in the separation factor or selectivity in a binary system. This effect is well depicted in Figure 5.3, where it is observed that the gas permeability of CO₂ and CH₄ get closer to each other with increasing pore size. This is because at larger pore size, the transport of gas molecules is predominated by Knudsen diffusion, which the selectivity between pure CO₂ and CH₄ is not as distinctive as the one under surface diffusion control. As mentioned earlier, CO₂ is much more strongly adsorbed by alumina compared to CH₄. Thus, the separation of

CO₂ / CH₄ binary system is more favoured at small pore size, where the surface diffusion predominates. This phenomenon will serve as an important point in future discussions. The cross observed in the trend is that in the Knudsen diffusion region, the lighter gas (CH₄) holds an advantage over the heavier gas (CO₂). Thus, CH₄ is said to permeate faster under Knudsen diffusion region, which is very not wanted for acid gas removal operation, as this results in loss of hydrocarbon.

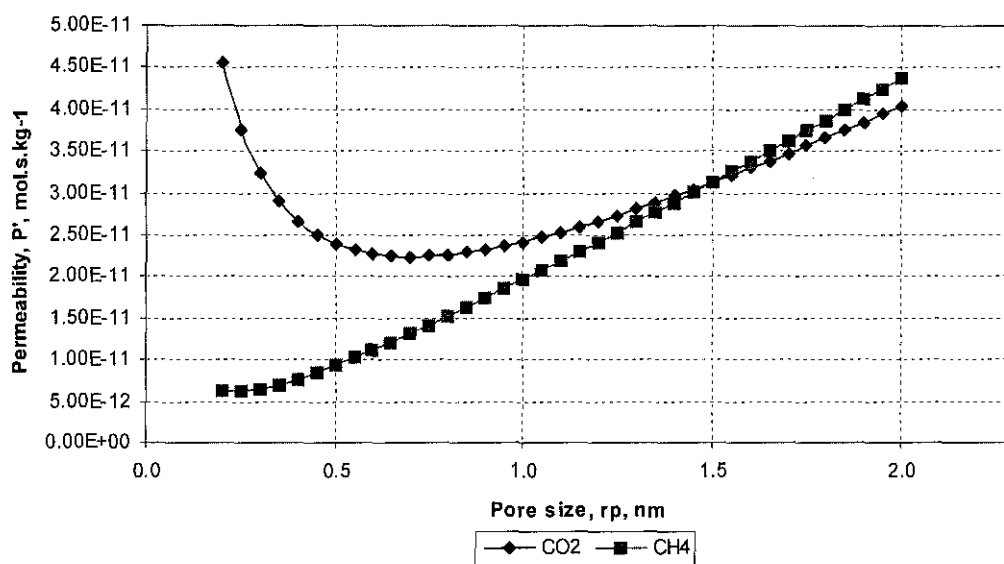


Figure 5.3: Effect of pore size on total permeability of CO₂ and CH₄ in γ -alumina membrane at T=303 K, P=60 atm.

5.1.2 Effect of Operating Pressure on Gas Permeability

The relationship of operating pressure and permeability of gas had been studied empirically by Suzuki, *et al.* (1987), Egan *et al.* (1992), Wu *et al.* (1993) and Cho *et al.* (1995) at pore size ranging from 3.5 nm to 7 nm. Their experimental results showed that permeability of gas is slightly or not really influenced by the operating pressure. A plot of gas permeability versus pressure yields an almost horizontal line.

However, it was found out that at small pore size (0.2 nm in this study), the total permeability of gas is quite dependent on operating pressure. Figure 5.4 shows that permeability of CO₂ increases with increasing operating pressure. As mentioned in

section 5.1.1, surface diffusion predominates Knudsen and viscous diffusion at small pore regions. Surface diffusion increases in this case primarily because of adsorption processes are favoured at high pressure due to increased molecular density. Same trend was observed for CH₄.

However, at bigger pore size, the permeability of CO₂ shows agreement with the experimental results by Suzuki, *et al.* (1987) and the others. This is because surface diffusion no longer predominates at larger pore regions and the dominant Knudsen diffusion is relatively independent of operating pressure. This is shown in Figure 5.5.

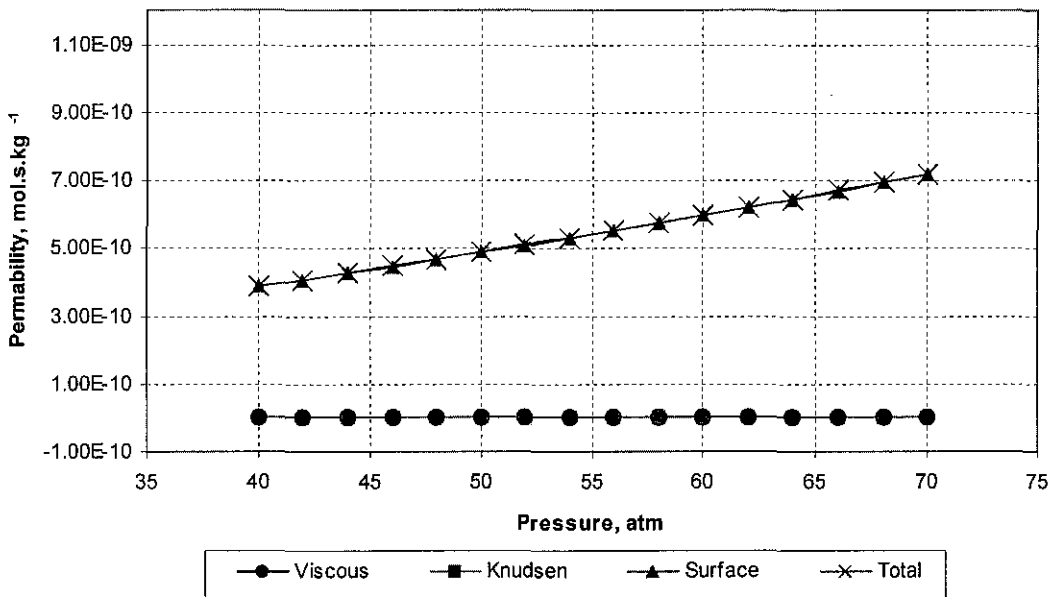


Figure 5.4: Effect of pressure on mechanism of flow for CO₂ in γ -alumina membrane at T=303 K, $r_p=0.2$ nm.

For CO₂ (Please refer to Figure 5.5), the permeability of gas at $r_p = 0.2$ nm lies between $r_p = 2$ nm and 4 nm. This can be explained by the strong adsorptivity nature of CO₂ gas, which is also shown in Figure 5.3 earlier on. For CH₄, as shown in Figure 5.6, operation at high pressure is believed to boost the permeation of the low adsorptive CH₄ gas. This can be observed that the permeation of CH₄ at $r_p = 0.2$ nm becomes more apparent than the one at $r_p = 1$ nm at pressures beyond 65 atm. However, operation at high pressure would mean that a bigger compressor is needed

to increase the feed pressure of the gas. This would be economic unattractive and on the other hand, operation dealing with extra high pressure is always risky.

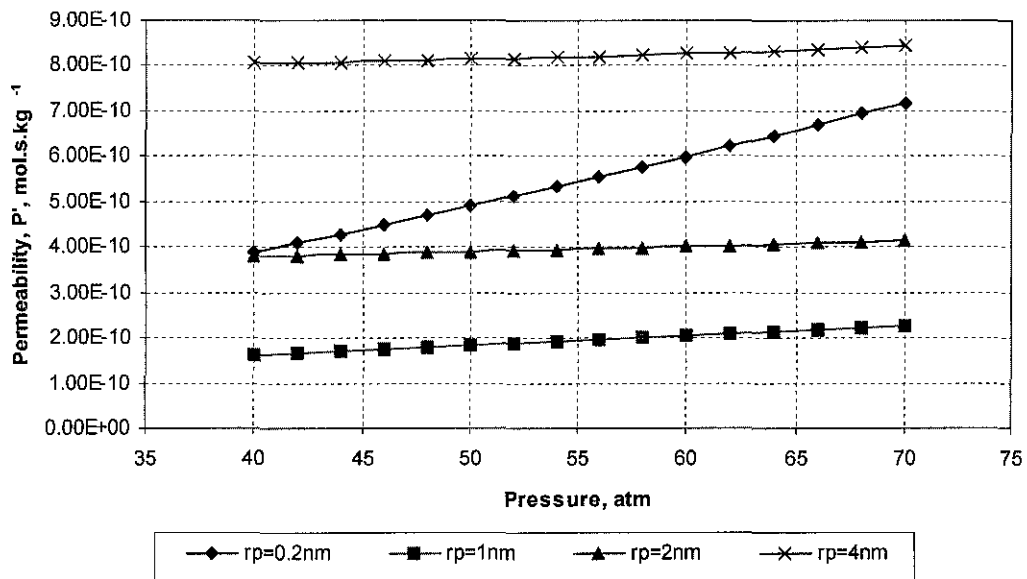


Figure 5.5: Effect of operating pressure on total permeability of CO₂ at different pore sizes in γ -alumina membrane at T=303 K.

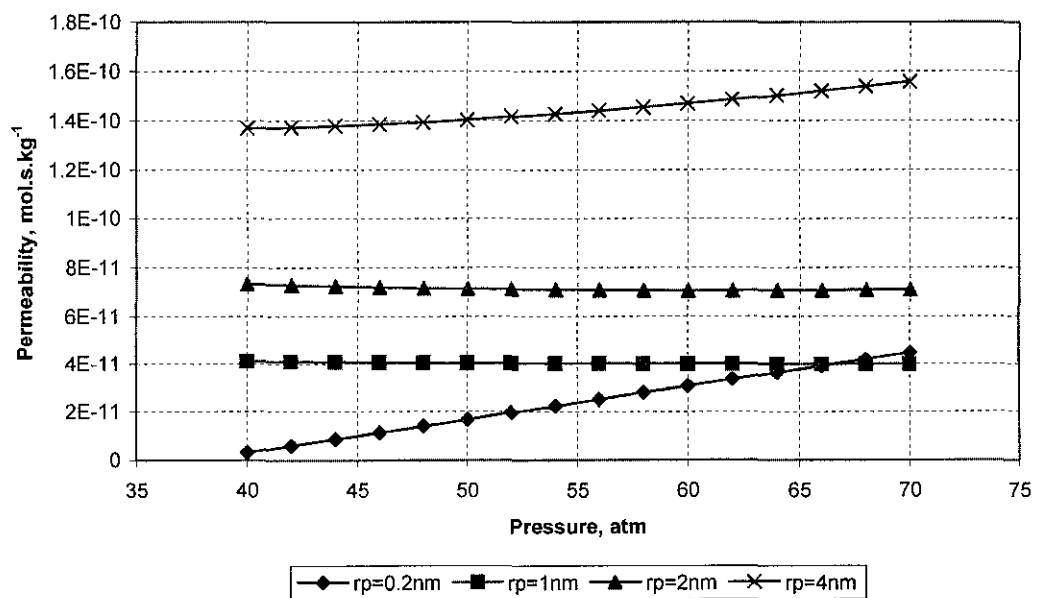


Figure 5.6: Effect of operating pressure on total permeability of CH₄ at different pore sizes in γ -alumina membrane at T=303 K.

5.1.3 Effect of Temperature on Gas Permeability

For gas permeation in porous membrane, permeability of gas is inversely proportional to the square root of temperature. This relationship was published by Cho *et al.* (1995), which documented his experimental work concerning the permeation of He, CO₂ and N₂ across γ -Alumina membrane.

The result of this study (in the region of $r_p=0.2$ nm) shows agreement with the theory cited earlier on. Figure 5.7 shows the effect of temperature towards the mechanism of flow for CH₄ permeation. It is observed that in this surface diffusion control region, the total permeability of CH₄ across membrane material decreases drastically with increasing temperature. This is because contribution of surface migration is due to adsorption, which the influence of temperature on adsorption can be described by using the thermodynamic relation between Gibbs free energy, enthalpy and entropy, $\Delta G = \Delta H - T\Delta S$. For adsorption process, ΔG is always negative, so do ΔH and ΔS . Hence, when temperature rises, ΔG becomes less negative and adsorption process is not favoured. The other two mechanisms namely Knudsen and viscous diffusion have not so obvious effect as the result of increasing temperature.

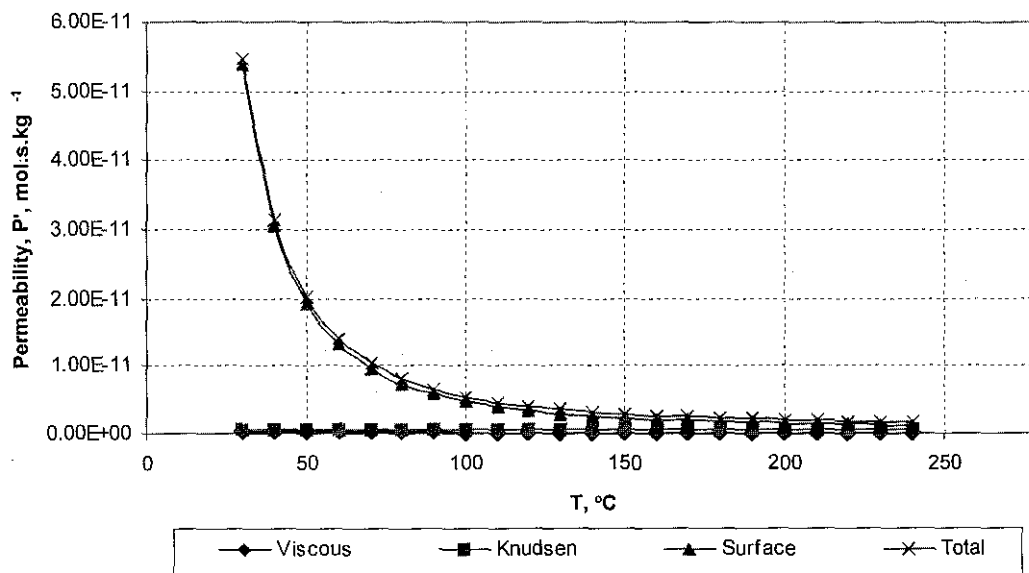


Figure 5.7: Effect of temperature on mechanism of flow for CH₄ in γ -alumina membrane at P=60 atm.

For membrane in different pore sizes, the total permeability of gas follows the general trend as proposed by Cho *et al.* (1995). As shown earlier, the permeability is higher at larger pore regions due to the higher availability of mean free pathways for the gas molecules. Figure 5.8 and 5.9 show the permeability of CH₄ and CO₂ at different pore sizes under the variation of temperature.

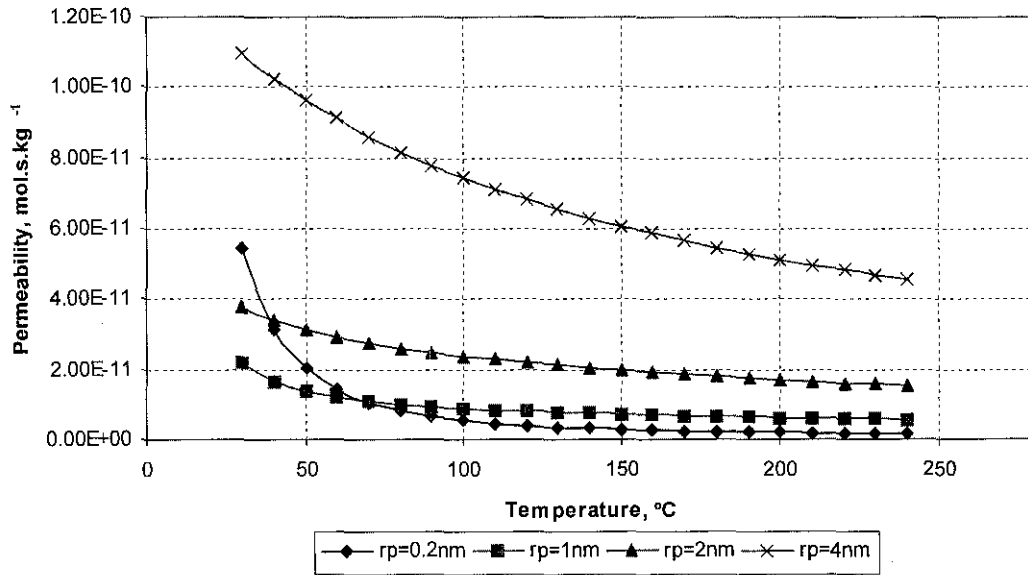


Figure 5.8: Effect of temperature on total permeability of CH₄ at different pore sizes in γ -alumina membrane at P=60 atm, $\varepsilon=0.603$, $\tau=1.658$, $t_m=0.1 \mu\text{m}$.

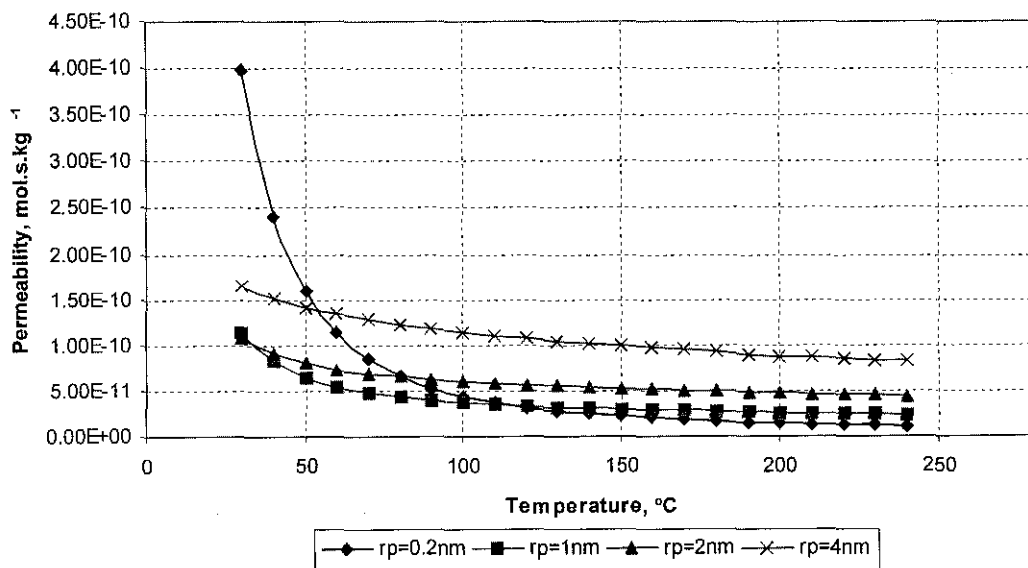


Figure 5.9: Effect of temperature on total permeability of CO₂ at different pore sizes in γ -alumina membrane at P=60 atm.

5.2 Pure Gas Permeability Versus Permeability of Gases in Binary Mixture

In studying the permeability of gas components in a mixture, the average viscosity and interaction between gas components need to be taken into account. In a gas mixture, the Knudsen diffusion and surface diffusion will behave the same as in pure gas system. This is because the basic principle for Knudsen diffusion is that the gas molecules will only collide with the pore walls rather than colliding with gas molecules either of the same species or different species. It is the ordinary diffusion of gases in a mixture that plays an important role due to the fact that different gas species have different affinity to each other and this will leave an impact on the permeation of different gas species in a mixture.

In this study, the pure gas permeability and the gas permeability of a binary mixture were compared under the same operating conditions at different pore sizes. At gas separation region, where $r_p=0.2$ nm, it is found that there is no difference between pure gas permeability and mixture's gas permeability upon variation in operating pressure, as can be seen in Figure 5.10. At small pore regions, the transports of both pure CO₂ and CH₄ are already restricted, not to mention the effects posed by the presence of other gas species. The only way for the gas molecules to pass through the membrane is by selective adsorption, depending on the type of membrane used (CO₂ is preferentially adsorbed on γ -alumina). No doubt that the mechanism of adsorption of CO₂ in a CO₂ / CH₄ mixture will be hindered by the presence of the latter, but the effect is negligibly small in small pore regions, as the gas molecules are already so close to the pore surface (Burggraaf and Cot, 1996). This explains why the pure gas permeability of both CO₂ and CH₄ are the same as in a mixture at small pore regions.

However, at larger pore size, which is 2 nm (as in Figure 5.11), the permeability of gas in mixture is found to be lower than the pure gas permeability, for both CO₂ and CH₄. This is a result of molecular interaction between the two different molecules. CH₄ is a larger molecule as compared to CO₂ in which it has a diameter of 3.8 angstroms compared to 3.3 angstroms for CO₂ (Bird *et al.*, 1960). In a mixture, CO₂ molecules will fill up the voids within CH₄ gas molecules. This will somehow

impede the transport of CH₄ across the membrane. On the other hand, being a faster diffusing gas as compared to CH₄ (Hsieh, 1996), the drop in transport of CO₂ molecules across the membrane can be described as the result of blocking effect by the bigger CH₄ molecules.

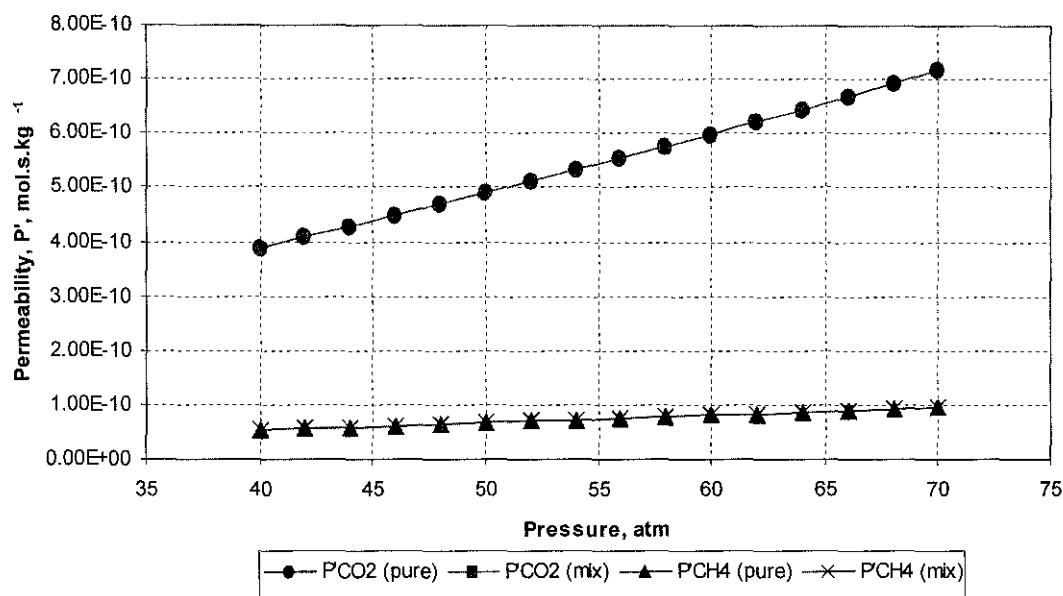


Figure 5.10: Pure gas permeability versus permeability of gas in mixture (20% CO₂ – 80% CH₄) in γ -alumina at $r_p=0.2$ nm, $T=303$ K.

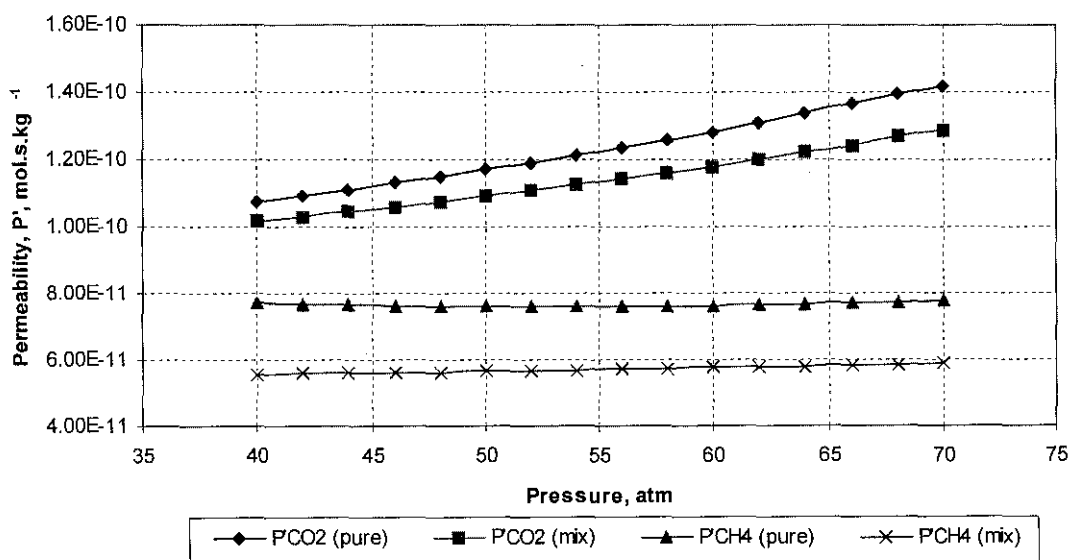


Figure 5.11: Pure gas permeability versus permeability of gas in mixture (20% CO₂ – 80% CH₄) in γ -alumina at $r_p=2$ nm, $T=303$ K.

Figure 5.12 and 5.13 show the effect of composition of CO₂ and CH₄ in the respective CO₂ / CH₄ mixtures. At larger pore sizes, it can be said that the gas permeability of CO₂ and CH₄ resembles more to their pure property as their composition in the mixture increases, approaching to 1.0.

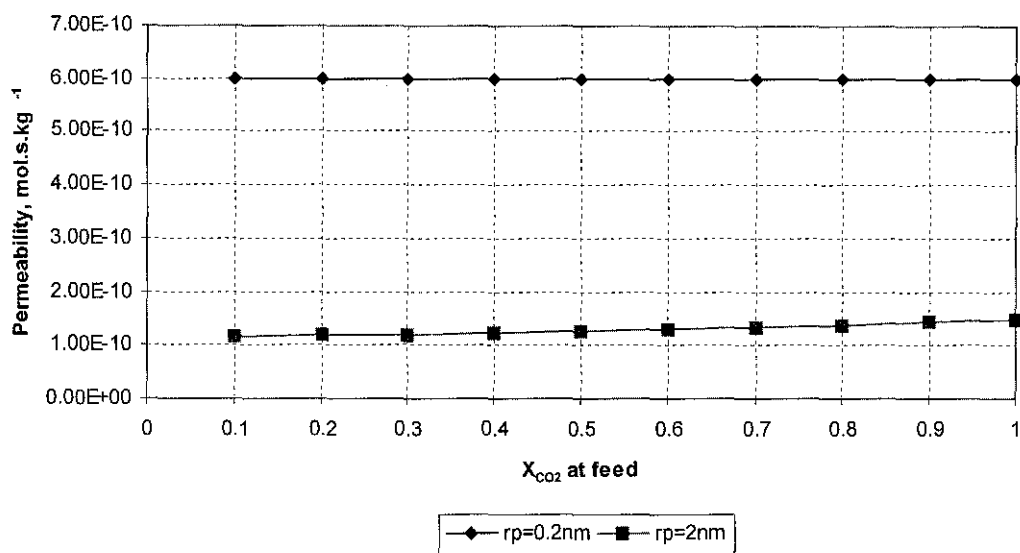


Figure 5.12: Gas permeability of CO₂ in CO₂ / CH₄ mixture as a function of feed composition at different pore size in γ-alumina membrane at P=60 atm, T=303 K.

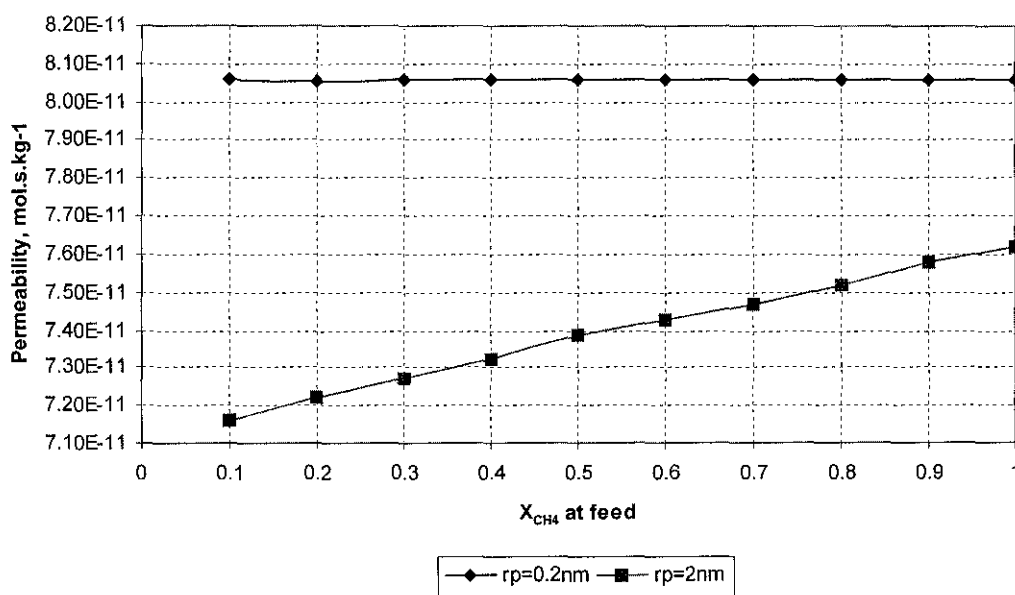


Figure 5.13: Gas permeability of CH₄ in CO₂ / CH₄ mixture as a function of feed composition at different pore size in γ-alumina membrane at P=60 atm, T=303 K.

5.3 Separation of CO₂ / CH₄ Binary System for High CO₂ Concentration

The most important aspect for binary gas mixture separation is the selectivity or separation factor. Higher separation factor would result in a sharper separation between the species in the binary mixture. In this study, the separation factor of CO₂ / CH₄ separation for high CO₂ concentration is studied based on the complete mixing model. The idea of using this model to predict the separation factor is that it is assumed that the gas species in the feed and permeate chamber are completely mixed, which is true in real application.

5.3.1 Effect of Operating Pressure and Pore Size on Separation Factor

In performing this study, the model is solved under the assumption that the membrane separator operates isothermally with negligible pressure drops in both feed and retentate streams. Typical industrial operating pressures (40 – 70 atm for feed pressure and normally 1 atm for permeate pressure) were obtained from Freeman and Pinnau (1999). Figure 5.14 shows the relation between separation factors at different pore sizes with respect to pressure ratio, which is defined as permeate pressure divided by feed pressure.

It is observed in Figure 5.14 that the separation of CO₂ / CH₄ mixture with 30% CO₂ in the feed does not really depend on the feed pressure. This is in accordance with the result as obtained from experimental works by Wu et al., (1993) and Cho et al., (1995). However, it is observed that the selectivity of this acid gas separation decreases with increasing pore sizes. This is because, at higher pore sizes, the separation is no longer predominated by surface diffusion, which is more selective due to difference in adsorptivity of different gas species. Now, the gas molecules have larger mean free pathways and other diffusions thus become easier. As a result, both gases can pass through the porous membrane easily and hence resulting in a lower separation factor.

Hwang and Kammermeyer (1975) reported that the economically justified separation factors in the industry for CO₂ removal is 3 – 50, depending on the types of

membrane used. It is shown in Figure 5.14 that separation of CO₂ from CH₄ at pore size greater than 2 nm will yield separation factors that are even lower than the Knudsen separation factor, which is the square root of the ratio of heavier component to lighter component. This suggests that the γ -alumina membrane, as the one used in this study should be manufactured to have pore size less than 1 nm for it to be economic and selective for CO₂ removal from CH₄.

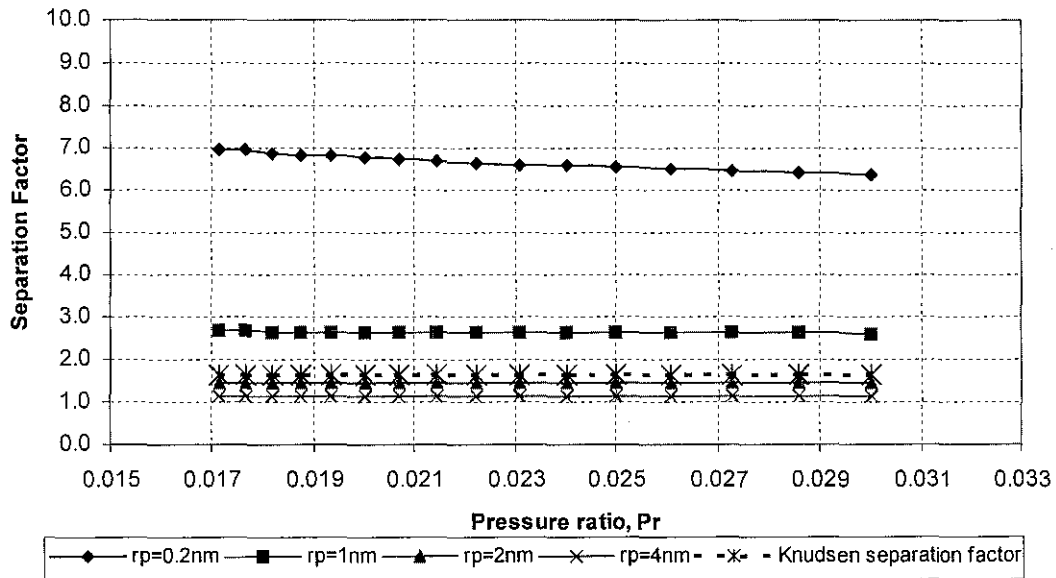


Figure 5.14: Effects of feed pressure on separation factor for CO₂ – CH₄ separation in γ -Alumina at different pore sizes, T=303 K, $x_f=0.30$, $\theta=0.206$.

5.3.2 Effect of Feed Concentration on Separation Factor

In Figure 5.15, the effect of feed concentration of CO₂ at pore size of 0.2 nm is studied as a function of pressure ratio. As the CO₂ concentration in the discussed CO₂ / CH₄ mixture decreases, the separation factor also decreases under selected operating conditions. This is because when the partial pressure (concentration) of CO₂ decreases, the number of CO₂ to CH₄ collisions increase relatively to that of the CO₂ to CO₂ collisions and consequently more CO₂ momentum is lost at low CO₂ concentration and the separation efficiency decreases. This is in accordance to the experimental results by Wu *et al.* (1993).

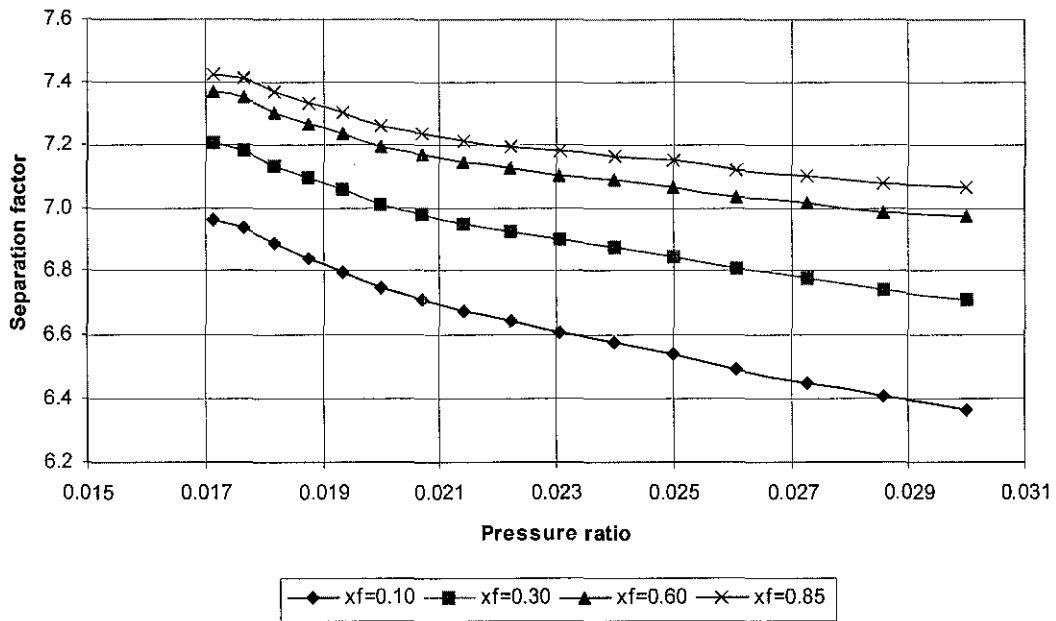


Figure 5.15: Effects of feed concentration on separation factor for CO₂ – CH₄ separation as a function of pressure ratio in γ -alumina at T=303 K, $r_p=0.2$ nm $\theta=0.206$.

5.3.3 Effect of Stage Cut on Separation Factor

Stage cut is defined as the ratio of permeate flow to feed flow rate. In Figure 5.16, the effect of stage cut at membrane pore size of 0.2 nm and feed concentration of 30 mole% is studied. It is found out that separation factor will decrease with increasing stage cut. At high stage cut (lower feed flow rate), the driving force for gas separation in terms of partial pressure difference (concentration gradient) is reduced to maintain the material balance (Burggraaf and Cot, 1996). Also, at lower feed flow rate, a longer contact time of the high – pressure residue gas with the active membrane area is achieved. This permits more CH₄ to permeate through the membrane material and thus a lower separation factor is obtained.

For CO₂ and CH₄ binary separation that occurs at higher pore sizes, same trends as in Figure 5.16 were observed and thus will not be presented here to avoid redundancy. The result of this study shows that the separation is enhanced by using a smaller stage cut, but the quality of the CH₄ gas collected at the retentate side, whether it meets the pipeline quality or not, is still not known at this stage. This will be discussed further in the proceeding sections.

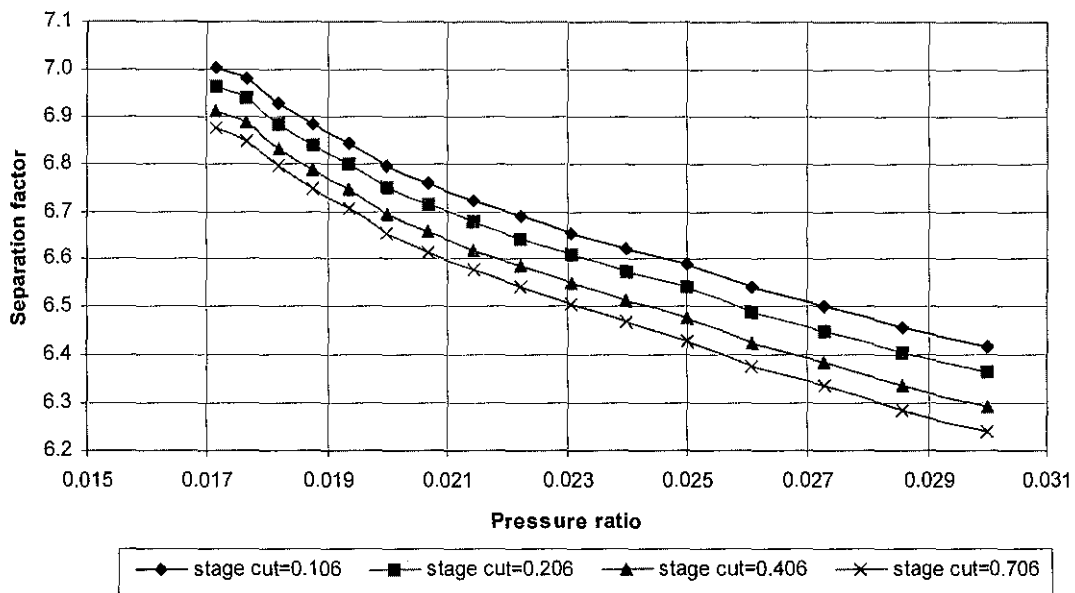


Figure 5.16: Effects of stage cut on separation factor for CO₂ – CH₄ separation as a function of pressure ratio in γ -alumina at T=303 K, x_f=0.3, r_p=0.2 nm.

5.3.4 Effect of Temperature on Separation Factor

For natural gas separation, particularly CO₂ removal, Coker *et al.* (1999) discussed in their work that the separation factor of CO₂ / CH₄ mixture increases when the system temperature decreases because the most permeable penetrant (CO₂) has the lower activation energy. On the other hand, Burggraaf and Cot (1996) mentioned that at higher temperature, the separation factor decreases because the mean free path increases and consequently more momentum loss is expected for the gas molecules. In this study, the effect of temperature towards the selectivity of the separation is investigated.

Figure 5.17 shows the trends of separation factor at different pore sizes as a function of temperature at an operating pressure of 60 atm. As expected, separations that take place at small pore regions (0.2 nm and 1 nm) have the highest separation factor followed by the separations that occur at larger pores (2 nm and 4 nm respectively). This phenomenon has been discussed in Section 5.1.1. However, it is most interesting to note the trends of the respective separation factors with variation in operating temperature.

For separation of CO₂ from CH₄ that occurs at surface diffusion control region (0.2 nm), the separation factor reaches a maximum and then decreases eventually as the operating temperature increases. As discussed in Section 5.1.3, the gas permeability of the gas components is inversely proportional to the square root of temperature. For separation in the surface diffusion control region, the permeability of the gas components will decrease at higher temperature as the result of reduced molecular density that does not favour the adsorption of the gas components on the pore surface. The energy supplied by the system at higher temperature will break the Van der Waals force that holds the adsorbed molecules on the pore wall surface. Thus, a steadily decrease in the separation factor is expected. However, careful study on the permeability data for both CO₂ and CH₄, it was revealed that the drop in permeability for CH₄ occurs in a greater extent as compared to CO₂ when the operating temperature increases from 30°C to 80°C. After the 80°C mark, the drop in individual permeability for CO₂ and CH₄ is more or less proportional. This is an interesting finding for CO₂ / CH₄ separation at small pore region at different temperatures.

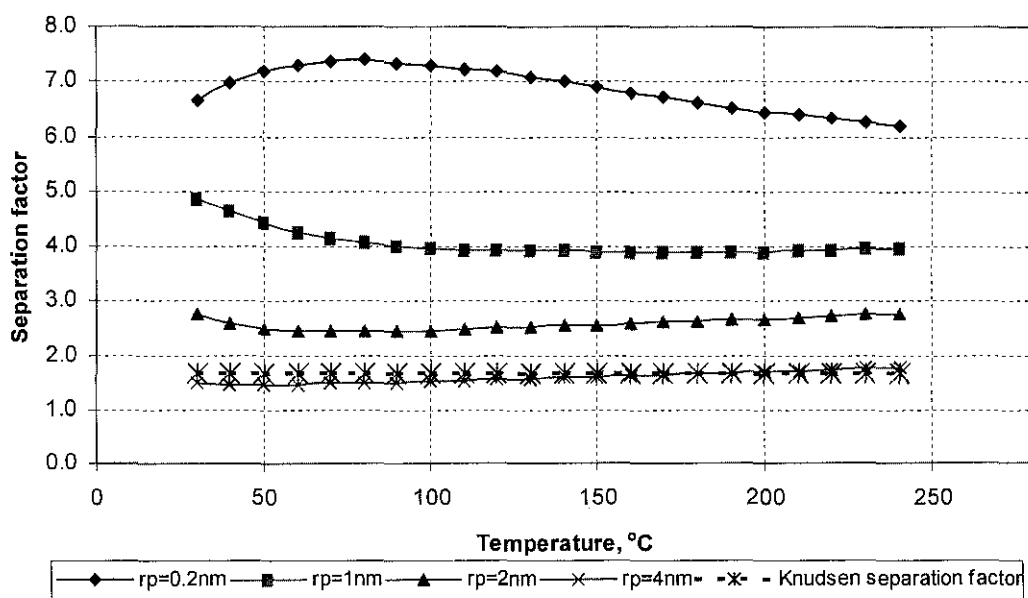


Figure 5.17: Effect of operating temperature on separation factors for CO₂ – CH₄ separation in γ -alumina at different pore sizes, P=60 atm, $x_f=0.3$.

Figure 5.18 shows the effect of feed concentration on the separation factor as a function of system temperature. It is again shown that the membrane is more efficient in term of selectivity at high CO₂ concentration, or simply higher partial pressure of CO₂ at the feed.

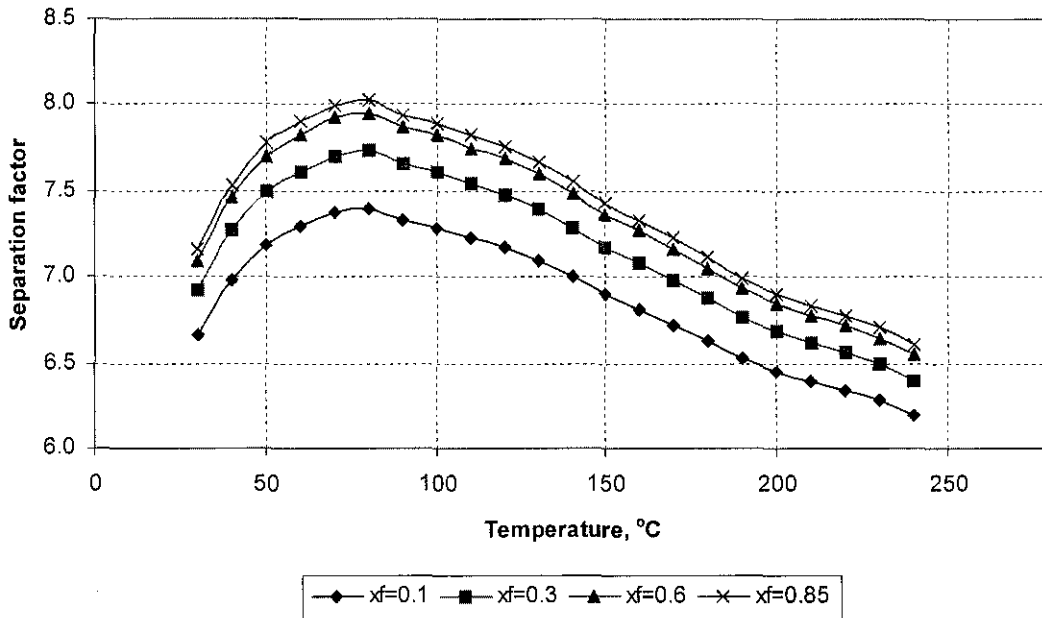


Figure 5.18: Effects of feed concentration on separation factor for CO₂ – CH₄ separation as a function of temperature in γ -alumina at P=60 atm, $r_p=0.2$ nm $\theta=0.206$.

5.3.5 Pipeline Quality of the Sale Gas

The behaviour of removal of high concentrated CO₂ from CH₄ has been looked into as a function of pressure, temperature, feed concentration and stage cut thus far, the quality of the CH₄ stream at the retentate side has not been carefully looked into. It is important to study the output from the membrane separation to see whether it achieves the pipeline quality for the sellable natural gas or not. Other operating conditions such as the effect of membrane area and thickness will not be studied, as membrane separators are insensitive to these effects (Seader and Henley, 1998).

As mentioned in Chapter 1, the typical specification of the treated natural gas calls for a CO₂ concentration of less than 2 mole% (Hsieh, 1996). It is thus the prime

objective in this section to study the compositions of CH_4 stream from the retentate side. All the study made in this project concern only single stage γ -alumina membrane separator with $\varepsilon=0.603$, $\tau=1.658$ and $t_m=0.1 \mu\text{m}$.

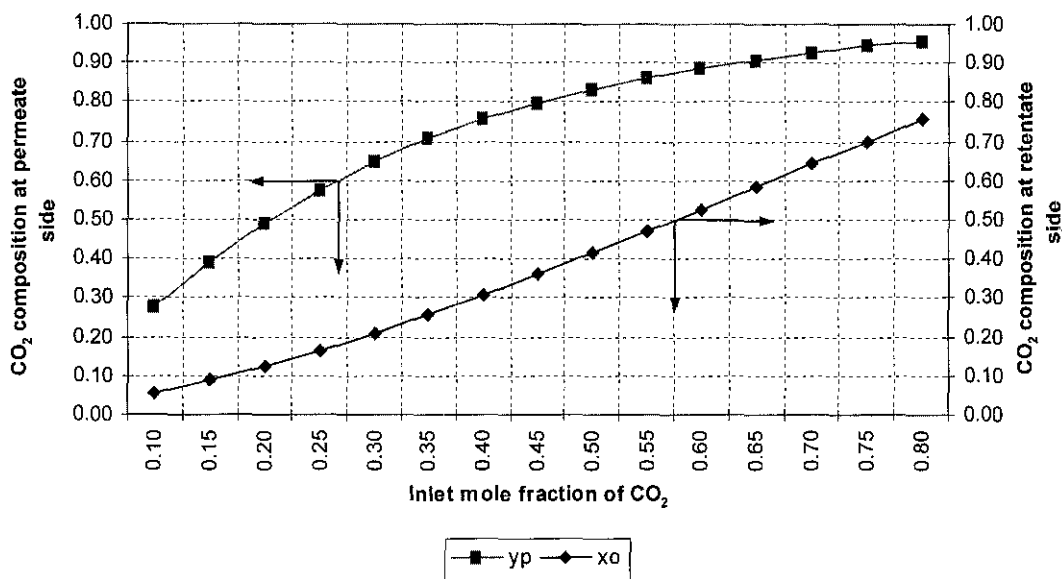


Figure 5.19: Variation of $y_{p\text{CO}_2}$ and $x_{o\text{CO}_2}$ as a function of feed composition of CO_2 in separation of $\text{CO}_2 - \text{CH}_4$ in γ -alumina membrane at $T=303 \text{ K}$, $P=60 \text{ atm}$, stage cut=0.206, $r_p=0.2 \text{ nm}$.

Figure 5.19 depicts the variation of the composition of CO_2 at both permeate and retentate sides across the Alumina membrane. It is expected that the increasing trends will be obtained when the feed composition of CO_2 is rising. This is because more CO_2 molecules are present in the membrane module when the feed composition increases. It is to note that the composition of CO_2 at the retentate stream is approximately 5 mole% when feed is fed with 10 mole% of CO_2 with a stage cut of 0.206. This is cry far higher than the pipeline quality of 2 mole%. This suggests that single membrane separator is not significant to remove the acid gas from the CH_4 stream at this stage cut. A higher stage cut would help to improve the quality of the CH_4 stream, where it registered approximately 2 mole% of CO_2 at the retentate side when stage cut 0.706 is used, as shown in Figure 5.20.

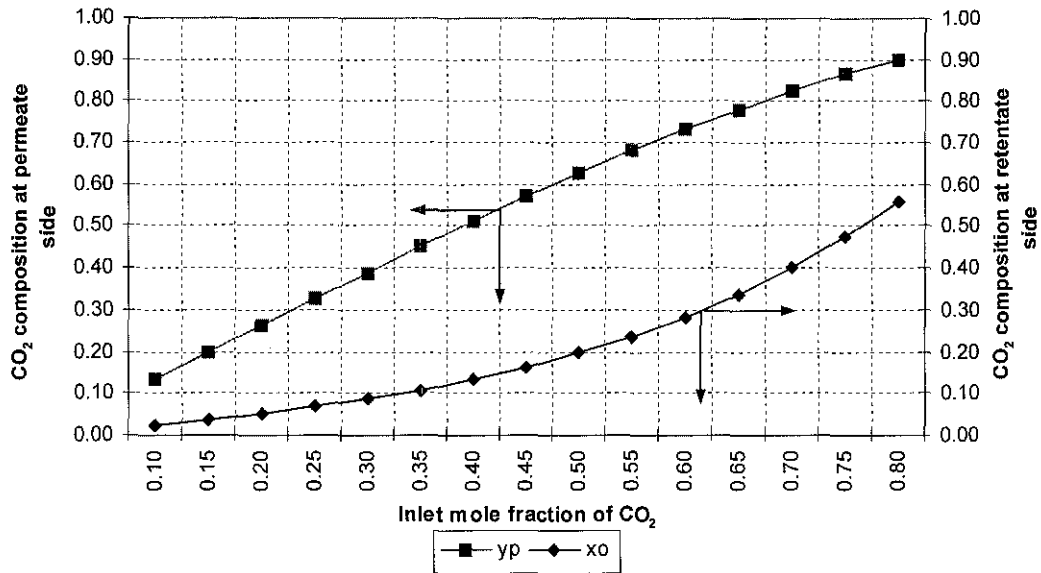


Figure 5.20: Variation of y_{pCO_2} and x_{oCO_2} as a function of feed composition of CO_2 in separation of $CO_2 - CH_4$ in γ -alumina membrane at $T=303$ K, $P=60$ atm, stage cut=0.706, $r_p=0.2$ nm.

However, it was discussed in Section 5.3.3 that higher stage cut would sacrifice a sharper separation in this binary system. Further investigation shows that it is only about 2.2% sacrifice (stage cut 0.706 vs. 0.206) in term of separation factor. In term of quality of the treated CH_4 stream, there is about 64% improvement in CO_2 removal as a whole. Figure 5.21 gives a clearer view.

The results presented suggests that by using a stage cut of 0.706, the system can produce a treated CH_4 stream with about 2 mole% from its original 10 mole% in the inlet. However, under the stage cut of 0.706 (lower feed flow rate), the loss of CH_4 to the permeate side is very huge, due to increased contact time of the high – pressure residue with the active membrane area (refer to Figure 5.21), which makes this operation mode unattractive in terms of economy. Thus, a lower stage cut in a cascaded manner would be economically justified. The cascading arrangement can also cater for this separation when a more concentrated CO_2 feed is fed to the membrane separator. It is of great interest to carry out study on the cascade arrangements for this binary separation in the future.

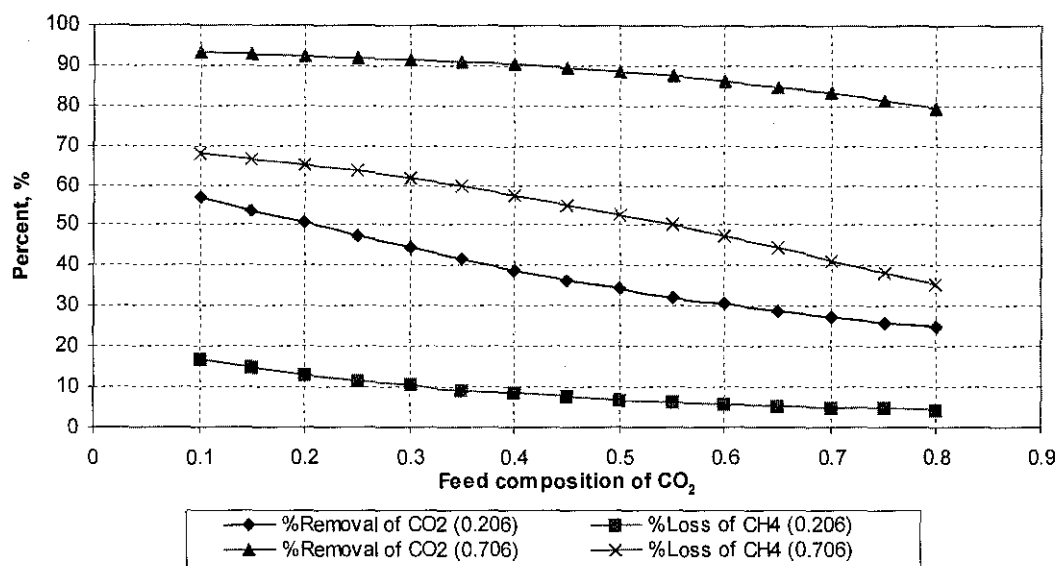


Figure 5.21: % removal of CO₂ and % loss of CH₄ at different stage cuts as a function of feed composition of CO₂ in CO₂ – CH₄ separation in γ -alumina membrane at T=303 K, P=60 atm, $r_p=0.2$ nm.

Echt (2002) mentioned that membrane separator is more efficient than amine absorber at high CO₂ inlet partial pressure. However, this couldn't be distinguished in this study due to lack of information on amine absorption and its outcomes in handling high content CO₂ natural gas.

5.4 Model Validation

The mathematical models developed have been used to study the behaviour of permeation of both CO₂ and CH₄ as well as the separation behaviour of this binary system. The question of how well can the model predict the actual scenario remains unanswered thus far. In this section, model validation is discussed where a set of experimental data (CO₂ / CH₄ separation using acetate cellulose membrane (Matsuura, 1993)) was fitted to the predicted curve, as shown in Figure 5.22.

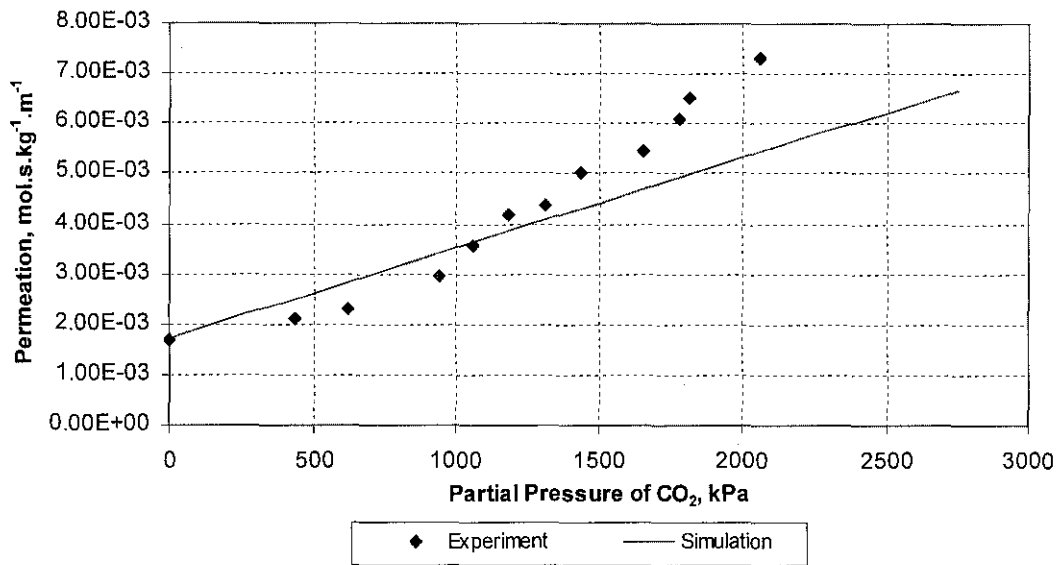


Figure 5.22: Comparison between model prediction and experimental data for CO₂ permeability on acetate cellulose membrane at T=305 K, stage cut=0.178, x_r=0.5

From Figure 5.22, it shows that the mathematical model developed in this study can predict the actual scenario of gas permeation reasonably up to 1700 kPa, the partial pressure of CO₂ in the system. The increasing trend of CO₂ permeability when pressure increases indicates the contribution of surface migration due to multilayer adsorption and diffusion. For simplicity in the model, these factors were not taken into consideration, as adsorption according to Henry's law was assumed. Further study reveals that for partial pressure range up to 1700 kPa, this model can make relatively accurate prediction with average absolute error of 2.70%.

For separation factor, the model managed to predict the separation with average absolute error of 12.07% with the experimental data, for data up to partial pressure range of 1700 kPa. When the system pressure continues to rise, the ability of the model in prediction becomes less accurate. Matsuura (1993) explains that the sharp drop in separation factor for CO₂ / CH₄ binary mixture at high pressure is mainly due to the plasticising effect of CO₂ on acetate cellulose membrane. Figure 5.23 shows the comparison between model prediction and experimental data for separation factor.

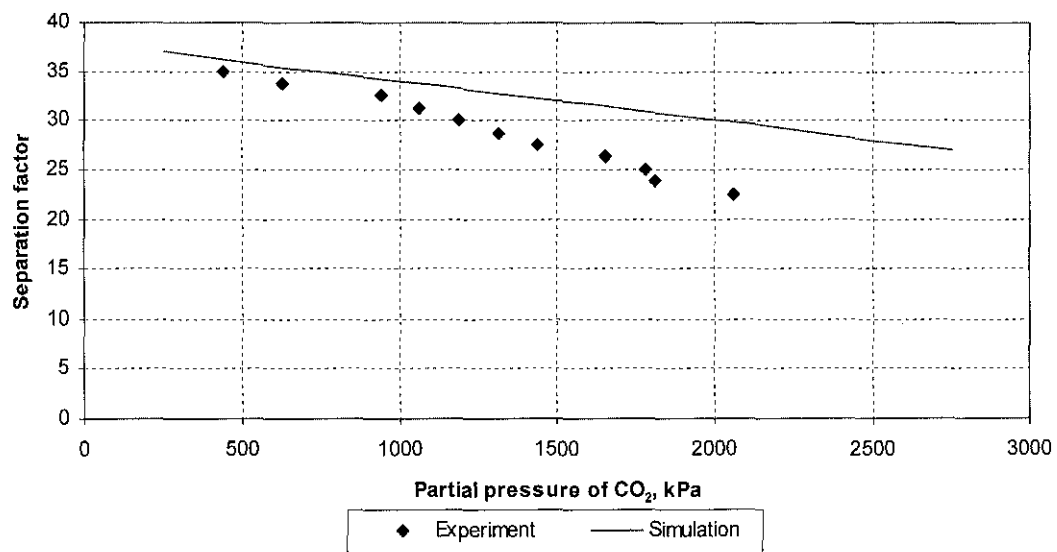


Figure 5.23: Comparison between model prediction and experimental data for CO₂ / CH₄ separation factor on acetate cellulose membrane at T=305 K, stage cut=0.178, x_r=0.5

CHAPTER 6

CONCLUSION AND RECOMMENDATION

The developed mathematical models are able to predict the transport of CO₂ and CH₄ gas molecules in γ -alumina and cellulose acetate membrane as well as the separation behaviour of this binary mixture with reasonably accuracy. The diffusion mechanisms due to viscous, Knudsen and surface play important roles in the transport of gas molecules across the membrane. This chapter will conclude the findings from various studies done by using the mathematical model. A few recommendations will also be presented at the end of this chapter for improvement in future works.

6.1 Conclusion

The first part of the study dealt with the study of gas permeability as a function of pore size. As we know, pore size plays an important role for mechanisms such as surface diffusion and Knudsen diffusion. The result shows that surface diffusion is favoured at small pore size (0.2 nm in this study) while Knudsen diffusion becomes apparent when the pore size increases as a result of increased mean free path of travel of the gas molecules. However, further increment of pore size would lead to unnecessary sacrifice in terms of selectivity of the separation process.

The effects of operating pressure and temperature on gas permeability were also looked into during this study. It was found out that at small pore size, the permeability of both CO₂ and CH₄ would increase as the operating pressure rises. This is due to the effect of pressure on surface diffusion, which predominates at small pore size. Adsorption process becomes more rigorous when operating pressure increases as a result of increased molecular density of the gas components. On the

other hand, Knudsen diffusion is not sensitive at all to operating pressure. Viscous diffusion is proportional to operating pressure, but its effect towards the total gas permeability is negligible at small pore size. At bigger pore sizes, where surface diffusion starts to lose its effect, the total permeability is relatively insensitive to operating pressure. Although viscous diffusion is a function of pressure, the effect is not that apparent in the Knudsen diffusion region.

For the effect of temperature, permeability of gas is inversely proportional to the square root of the system temperature. The result of this study tallies with the theory cited earlier. This is because the adsorption of gas molecules on the membrane pore wall surface becomes less. This effect is the most obvious at small pore region, where surface diffusion is a strong function of system temperature.

In studying the permeability of gas components in a mixture, the viscosity of the mixture and the effect of molecular interaction between the gas molecules should be taken into account. For gas in the mixture, Knudsen diffusion and surface diffusion behaves exactly the same as in the pure condition. It is the ordinary diffusion that plays an important role, as different gas species will have different affinity towards each other. This affects the transport of different gas species in a mixture.

For the study carried out at small pore size (0.2 nm), it was found out that the pure gas permeability overlaps the permeability of gas in a mixture. This is mainly due to that surface diffusion takes control at small pores. However, at higher pore size (2 nm), the permeability of both CO₂ and CH₄ are found to be lower than the ones in the pure condition, due to different interaction between the gas species. The gas permeability of CO₂ and CH₄ in CO₂ / CH₄ mixture will approach the pure gas permeability as the feed composition of the gas increases, and vice versa.

After obtaining the full understanding of the transport mechanisms of CO₂ and CH₄ in the membrane as a function of different process variables, the project was continued with the study of the separation behaviour of this binary mixture as a function of different process parameters. It is important to study the separation factor of the binary system, as it is the tool to determine the cost effectiveness of a separation.

The separation factors of this binary mixture were studied by employing the complete mixing model with the assumption that complete mixing occurs in both the feed and permeate chamber, and that the retentate stream exits with negligible pressure drop. It was observed that the separation of CO₂ – CH₄ with 30% CO₂ in the feed is insensitive to the operating pressure. It was also observed that the separation factor decreases with increasing pore size. This is because the membrane separator becomes unselective at bigger pore size, as both the CO₂ and CH₄ molecules have bigger mean free path of travel. An important finding was that separation that takes place at pore size bigger than 2 nm perform even worse than the Knudsen separation factor, which is about 1.66 for CO₂ / CH₄ mixture.

The effect of feed concentration of CO₂ in this binary system was also investigated. The study revealed that the separation is enhanced greatly when more CO₂ is present at the feed. This is because the CO₂ molecules gain more momentum as a result of collision between the same species in the pore.

Stage cut does play a prominent role in this binary separation. The effect of stage cut on the separation performance was studied and the result showed that increased stage cut would make the separation unattractive in term of separation performance. This is because at higher stage cut (lower feed flow rate), the contact time of high – pressure residue with the active membrane area is longer and thus permitting more CH₄ to permeate through the membrane material. This results in higher loss of CH₄ to the permeate stream.

Temperature is an important parameter in any separation processes. The result of this study showed that at pore size of 0.2 nm, the separation factor would reach a maximum before decrease gradually. This is because the drop in permeability for CH₄ occurs at a bigger extent as compared to CO₂ at higher temperature due to increased molecular density. This explains that the separation of CO₂ from CH₄ is actually enhanced at suitable temperature range although the individual gas permeability reduces when temperature rises. At bigger pore size, where surface diffusion loses its effect, the separation is slightly enhanced as a result of increased energy level for the diffusing gas.

The pipeline quality of the treated CH₄ stream was also investigated at pore size equals to 0.2 nm. It was found out that a stage cut of 0.206 will reduce the composition of CO₂ in the CH₄ stream to 5 mole% from the initial 10 mole%, in a single staged membrane separator. The composition of CO₂ in the CH₄ stream can be reduced to 2 mole% (the typical pipeline specification) with a stage cut of 0.706. However, this high stage cut value infers the severity of loss of CH₄ in the retentate stream, which makes this configuration unattractive in term of economics.

Lastly, the model validation shows that the models developed help to predict the permeability of gas and separation behaviour of removal of CO₂ from CH₄ with reasonable accuracy. The results also show that the model is not so accurate at high partial pressure of CO₂ due to the effect of multi layer diffusion and high plasticising effect of CO₂ on the Acetate cellulose membrane. These two parameters are not yet incorporated in the current models developed.

6.2 Recommendations

The mathematical models developed in this project have helped to study the behaviour of gas permeation in porous membrane as well as the separation behaviour of CO₂ / CH₄ binary system. However, there are still many more studies that can be extended from this endeavour to improve the models developed. Illustrated next are a few extended studies that are recommended:

1. Series of experiment can be carried out to study the validity of the mathematical models developed in this study. Necessary tuning of the models can be done in order to improve the reliability of these models. The results predicted from this modelling work can also be compared with other empirical models such as the Dusty Gas Model and the extended P – D model, as discussed in chapter 2.
2. The flow pattern used in this project to study the performance of separation was complete mixing model. It is recommended that future work can focus on the counter current flow model as it is claimed to be the most practical and cost effective method in the industry. Nevertheless, the other two flow models namely

cross flow model and co – current flow model can also be studied to compare their efficiency.

3. This modelling work employed only single staged membrane separator. It is thus a need for future researchers to study the various sequencing methods of membrane separator to derive a suitable model for effective membrane separation.
4. An example of surface diffusion – driven separation is CO₂ through the pores of γ -Alumina (Hsieh, 1996). At a relatively low temperature and high pressure, some gases will undergo capillary condensation (multilayer adsorption), when the adsorbed molecules form layers on top of each other and eventually condense and clog the pores of the membrane. It is strongly recommended that the effect of capillary condensation could be taken into account for future studies, as it plays an important role under certain operating conditions. This effect is best seen in Section 5.4, where the model prediction is no way to be close to that of the experimental data when system pressure continues to rise.
5. CO₂ is known to have plasticising effect on certain organic membranes at high pressure. This effect would affect the separation performance of CO₂ / CH₄ binary system. The incorporation of a model that takes into account of plasticising effect of gas on organic membrane would add more scientific values to the existing model.
6. The existing models developed assumed an isothermal operation in the membrane module. Heating and cooling can occur in the membrane module due to Joule – Thompson expansion effect. It is recommended that future works could take into account of this effect as work by Gorissen (1987) showed that there is large difference (approximately 30°C) in the exit temperature for CO₂ / CH₄ separation as compared to ideal condition.
7. It is assumed, for simplicity, in this study that the pore size does not expand when the temperature rises. Under severe temperature, the expansion in pore

mouths will more or less influence the mechanism of gas permeation in porous membrane. It is suggested that future work could take this effect into account.

REFERENCES

1. **Arnold, K. and Stewart, M.**, 1989, *Surface Production Operations. Design of Gas – Handling Systems and Facilities*, Gulf Publishing Co., Houston
2. **Atkins, P.W.**, 1994, *Physical Chemistry*, 5th edition, Oxford University Press, London, p.37, 40 & 824
3. **Bird, R.D., Stewart, W.E. and Lighfoot, E.N.**, 1960, *Transport Phenomena*, 4th edition, John Wiley and Son, New York
4. **Blaisdell, C.T., and Kammermeyer, K.**, 1973, “ Isothermal Modelling for Membrane Separation,” *Chem. Eng. Sci.* 28: 1249
5. **Bugrraaf, A.J. and Cot, L.**, 1996, *Fundamentals of Inorganic Membrane Science and Technology*, Elsevier, Amsterdam
6. **Cho, Y.K., Han, K. and Lee, K.H.**, 1995, “Separation of CO₂ by Modified γ - alumina Membranes at High Temperature,” *J. Mem. Sci.*, 104: 219 - 230
7. **Coker, D.T., Allen, T., Freeman, B.D., and Fleming, G.K.**, 1999 “Non-isothermal Model for Gas Separation Hollow-Fiber Membranes,” *AICHE Journal* 45: 1451
8. **Cooley, T.E.**, 1990, “The use of membranes for natural gas purification,” *Proc.-Eur.Ch.Cont.Meet.-Gas Process.Assoc.*, Biarritz, FRA, May 17-18, p.17
9. **Cornelissen, A.E.**, 1993 “Heat Effect in Gas Permeation, with Special Reference to Spiral-Wound Modules,” *J. Memb. Sci* 76: 185
10. **Cunningham, R.E. and Williams, R.J.J.**, 1980, *Diffusion in Gases and Porous Media*, Plenum Press, New York
11. **Echt, W.**, 2002, “Hybrid Systems: Combining Technologies Leads to More Efficient Gas Conditioning”, *Laurance Reid Gas Conditioning Conference*, www.uop.com
12. **Eickmann, W. and Werner, U.**, 1985, “Gas separation using porous membranes”, *Ger. Chem. Eng.*, 8, 186-194

13. **Egan, B.Z., Fain, D.E., Roettger, G.E. and White, D.E.**, 1992, "Separating Hydrogen from Coal Gasification Gases with Alumina Membranes", *J. Eng. G. T. and P.*, 114, p.367-370
14. **Freeman, B.D. and Pinnau, I.**, 1999, *Polymer Membranes for gas and Vapour Separation*, Oxford University Press, USA
15. **Gas Malaysia Sdn. Bhd.**, 2003
16. **Genkopolis, C.J.**, 1993, *Transport Processes and Unit Operations*, 3rd edition, Prentice Hall PTR, New Jersey
17. **Gorissen, H.**, 1987 "Temperature Changes Involved in Membrane Gas Separations," *Chem. Eng. Process* 22: 63
18. **Hsieh, H.P.**, 1996, *Inorganic Membranes for Separation and Reaction*, Elsevier, Amsterdam
19. **Johnston, I.W., King, M.**, 1987, "An introduction to membrane technology and the role of membrane in gas processing," *Unit Operations in Offshore and Onshore Production*, Proc.-IchemE Subj. Group Oil nature, Gas-Gas Process. Assoc. Eur. Meet., Aberdeen, GBR, June 18-19, p.37-53
20. **Keizer, K., Uhlhorn, R.J.R., Van Varen, R.J. and Burggraaf, A.J.**, 1988, "Gas Separation Mechanism in Microporous Modified γ -Alumina Membrane", *J. Memb. Sci.*, 39, p.285-300
21. **Krevelen, D.W.Van**, 1990, *Properties of Polymers*, Elsevier, Amsterdam,
22. **Lee, K.H., and Hwang, S.T.**, 1985, "The Transport of Condensable Vapours Through a Microporous Vycor Glass Membrane," *J. Col. And Inter. Sci.*, 110: 544 - 555
23. **Mason, E.A., Malinauskas, A.P. and Evans, R.B.**, 1983, *Gas Transport in Porous Media: The Dusty Gas Model*. *Cehm. Eng. Mon.*, 17. Elsevier, Amsterdam
24. **Meyer, M., Renesme, G., Brefort, B.**, 1991, "The processes of gas separation by permeation through polymeric membranes: present and future potential in the gas industry," *Recl. Communic. 108e Congr. Gaz*, Montpellier, FRA, September 17-21 (2): 3-54
25. **Matsuura, T.**, 1993, *Synthetic Membranes and Membrane Separation Processes*, CRC, USA.

26. **Osada, Y.**, and **Nakagawa, T.**, 1992, *Membrane Science and Technology*, Marcel Dekker, Inc., New York, p.239-288
27. **Othman, M.R.**, 2001, *Kajian Pemisahan Gas Pada Membrane – membrane Tak Organik Terubahsuai*, Ph.D. Thesis, USM, Malaysia
28. **Perry, R.H.**, and **Green, D.W.**, 1997, *Perry's Chemical Engineers' Handbook*, 7th edition, McGraw-Hill International Editions, New York, p.22-61
29. **Present, R.D.** and **De Bethune, A.J.**, 1949, "Separation of a gas mixture through a long tube at low pressure", *Phys. Rev.*, 75, 1050-1057
30. **Rautenbach, R.**, and **W. Dahm**, 1987, "Gas Permeation – Module Development and Arrangement," *Chem. Eng. Process* 21: 141
31. **Rogers, C.E.**, 1985, *Physics and Chemistry of the Organic Solid State*, Interscience, New York.
32. **Roje, A.**, **Jaffret, C.**, **Cornot – Gandolphe, S.**, **Durand, B.**, **Jullian, S.** and **Valais, M.**, 1997, *Natural Gas Production Processing Transport*, Editions Technip, Paris
33. **Rouquerol, J.**, **Avnir, D.**, **Fairbridge, C.W.**, **Everett, D.H.**, **Haynes, J.H.**, **Pernicone, N.**, **Ramsay, J.D.F.**, **Sing, K.S.W.** and **Unger, K.K.**, 1994, "Recommendations for the characterisation of porous solids," *Pure Appl. Chem.*, 66: 1739 - 1758
34. **Seader, J.D.**, and **Henley, E.J.**, 1998, *Separation Process Principles*, John Wiley and Sons, Inc., New York, p.713-773
35. **Spillman, R.W.**, 1989, *Chem. Eng. Progr.* 85, p. 41.
36. **Spillman, R.W.**, and **M.B. Sherwin**, June 1990, " Membrane in Life," *Chemtech*: 378-384
37. **Stastna, J.** and **De Kee, D.**, 1995, *Transport Properties in Polymers*, Technomic Publishing, Lancaster, USA
38. **Suzuki, F.**, **Onozato, K.** and **Kurokawa, Y.**, 1987, "Gas Permeability of a Porous Alumina Membrane Prepared by The Sol – Gel Process", *J. Non-Crys. Solids*, 94, p.160-162
39. **Treybal, R.E.**, 1981, *Mass Transfer Operation*, 3rd ed., McGraw Hill Book Company, Boston
40. **Uhlhorn, R.J.R.**, 1990, *Ceramic Membranes for Gas Separation*, Ph.D. Thesis, University of Twente, Enschede, The Netherlands

41. **Uhlhorn, R.J.R.** and **Burggraaf, A.J.**, 1990, *Gas Separation with Inorganic Membranes*, in: Bhave, R.R. (Ed.), *Inorganic Membranes*. Van Nostrand Reinhold, New York, p. 155 - 176
42. **Veldsink, J.W.**, 1993, *A Catalytically active, non permselective membrane reactor for kinetically fast, strongly exothermic heterogeneous reactions*, Ph.D Thesis, University of Twente, The Netherlands
43. **Vieth, W.R.**, 1991, *Diffusion in and Through Polymers*, Hanser Publishers, Germany
44. **Walawender, W.P.**, and **Stern, S.A.** 1972, "Isothermal Membrane Modelling," *Sep. Sci.* 7: 553
45. **Weller, S.**, and **Steiner, W.A.**, 1950 "Modelling of Membrane Separation," *Chem. Eng. Progr.* 46: 585
46. **Wu, J.C.S.**, **Flowers, D.F.** and **Liu, P.K.T.**, 1993, "High Temperature Separation of Binary Gas Mixtures Using Microporous Ceramic Membranes", *J. Memb. Sci.*, 77, p.85-98

Appendix A: Properties of CO₂ and CH₄

Properties	CO ₂	CH ₄
M.W	44.01	16.04
Kinetic diameter, Å	3.40	3.88
T _c , K	304.10	190.60
P _c , Bar	73.80	46.00
T _{nbp} , K	194.50	111.60
v _c , cc/mol	93.90	99.00
ω	0.23	0.01
z _c	0.27	0.29
ΔH_{ads} at standard, kJ/mol	25.24	8.18
Density, kg/m ³	1.80	0.66

Appendix B: Compressibility factors of CO₂

T (°C)	Pressure (Bar)							
	1	5	10	20	40	60	80	100
0	0.9933	0.9658	0.9294	0.8496				
50	0.9964	0.9805	0.9607	0.9195	0.8300	0.7264	0.5981	0.4239
100	0.9977	0.9883	0.9764	0.9524	0.9034	0.8533	0.9022	0.7514
150	0.9985	0.9927	0.9853	0.9705	0.9416	0.9131	0.8854	0.8590
200	0.9991	0.9953	0.9908	0.9818	0.9640	0.9473	0.9313	0.9170
250	0.9994	0.9971	0.9943	0.9886	0.9783	0.9684	0.9593	0.9511
300	0.9996	0.9982	0.9967	0.9936	0.9875	0.9822	0.9773	0.9733
350	0.9998	0.9991	0.9983	0.9964	0.9938	0.9914	0.9896	0.9882
400	0.9999	0.9997	0.9994	0.9989	0.9982	0.9979	0.9979	0.9984

Appendix C: Compressibility factors of CH₄

T (°C)	Pressure (Bar)							
	1	5	10	20	40	60	80	100
50	0.9854	0.9225	0.8275	0.7740	0.7431	0.7093	0.6763	0.6423
100	0.9936	0.9676	0.9339	0.8599	0.7784	0.7559	0.7172	0.7618
150	0.9965	0.9838	0.9680	0.9352	0.8682	0.8020	0.7386	0.7854
200	0.9983	0.9915	0.9839	0.9667	0.9343	0.9047	0.8783	0.8556
300	0.9991	0.9954	0.9911	0.9825	0.9662	0.9520	0.9401	0.9306
400	0.9995	0.9977	0.9953	0.9912	0.9835	0.9772	0.9726	0.9696

Appendix D: Lennard – Jones parameters for CO₂ (Bird *et al.*, 1960)

T, °C	kT / ε	Ω_{μ}
20	1.5421	1.2988
28	1.5842	1.2844
30	1.5947	1.2808
100	1.9632	1.1831
150	2.2263	1.1338
200	2.4890	1.0945
250	2.7256	1.0632
300	3.0158	1.0376
350	3.2789	1.0157
400	3.5421	0.9971
450	3.8053	0.9808
500	4.0684	0.9665

Appendix E: Lennard – Jones parameters for CH₄ (Bird *et al.*, 1960)

T, °C	kT/ϵ	Ω_μ
30	2.212	1.1361
100	2.723	1.0665
150	3.088	1.0311
200	3.453	1.0032
250	3.818	0.9801
300	4.182	0.9609
350	4.547	0.9444
400	4.912	0.9301
450	5.277	0.9184
500	5.642	0.9073
550	6.007	0.8961
600	6.372	0.9975

Appendix F: Mathcad Programming Samples

Study of gas permeability as a function of pore size.

$i := 1, 2.. 20$

$r_i := 0.2 \cdot 10^{-9} \cdot i$

1. **INPUT** the desired pore size range

$T := 303$

$P := 60$

2. **INPUT** the desired operating temperature and pressure

$\epsilon := 0.603$

$\tau := 1.658$

3. **INPUT** the properties of the membrane ϵ is porosity, τ is tortuosity
 t_m is membrane thickness, ρ_m is membrane density

$t_m := 0.1 \cdot 10^{-6}$

$\rho_m := 3040$

$M1 := 44.01$

$M2 := 16.043$

$\sigma 1 := 3.3$

4. **INPUT** the properties of the gas components. 1 for Carbon Dioxide,
 2 for Methane. M is molecular weight, σ is diameter,
 Ω is Lennard-Jones parameter, ΔH is heat of adsorption, f is
 adsorption uptake on the membrane material

$\sigma 2 := 3.88$

$\Omega 1 := 1.2988$

$\Omega 2 := 1.1361$

$\Delta H 1 := -17116$

$\Delta H 2 := -21000$

$f 1 := 0.0000618$

$f 2 := 0.0000215$

$$\mu 1 := 2.6693 \cdot 10^{-5} \cdot \frac{\sqrt{M1 \cdot T}}{\sigma 1^2 \cdot \Omega 1} \cdot \frac{100}{1000}$$

5. **CALCULATE** viscosity of the gas components

$$\mu 2 := 2.6693 \cdot 10^{-5} \cdot \frac{\sqrt{M2 \cdot T}}{\sigma 2^2 \cdot \Omega 2} \cdot \frac{100}{1000}$$

$$P_{vis1_i} := \epsilon \cdot \frac{\left(r_i\right)^2 \cdot \left(\frac{P + 1.2}{2}\right)}{8 \cdot \tau \cdot \mu 1 \cdot 0.7515 \cdot 82.06 \cdot T \cdot \frac{1}{10^6}}$$

6. **CALCULATE** permeability due to viscous diffusion
 0.7515 as the compressibility factor
 for CO2 at the operating condition,
 0.9758 is for CH4

$$P_{vis2_i} := \epsilon \cdot \frac{\left(r_i\right)^2 \cdot \left(\frac{P + 1.2}{2}\right)}{8 \cdot \tau \cdot \mu 2 \cdot 0.9758 \cdot 82.06 \cdot T \cdot \frac{1}{10^6}}$$

$$Dk1_i := \frac{2 \cdot \left(r_i - \frac{0.33 \cdot 10^{-9}}{2} \right) \cdot \sqrt{\frac{8 \cdot 8.314 \cdot 1000 T}{3.142 \cdot M1}}}{3}$$

7. CALCULATE knudsen diffusivity

$$Dk2_i := \frac{2 \cdot \left(r_i - \frac{0.33 \cdot 10^{-9}}{2} \right) \cdot \sqrt{\frac{8 \cdot 8.314 \cdot 1000 T}{3.142 \cdot M2}}}{3}$$

$$Pk1_i := \frac{\varepsilon \cdot \left(\frac{1}{\frac{1}{1.723 \cdot 10^{-5}} + \frac{1}{Dk1_i}} \right)}{0.7515 \cdot \tau \cdot 82.06 \cdot \frac{101325}{1 \cdot 10^6} \cdot T}$$

8. CALCULATE permeability due to Knudsen diffusion

$$Pk2_i := \frac{\varepsilon \cdot \left(\frac{1}{\frac{1}{1.723 \cdot 10^{-5}} + \frac{1}{Dk2_i}} \right)}{0.9758 \cdot \tau \cdot 82.06 \cdot \frac{101325}{1 \cdot 10^6} \cdot T}$$

$$Ds1 := \frac{1.62 \cdot 10^{-2}}{1 \cdot 10^4} \cdot 2.712 \cdot \frac{-0.45 \cdot (-\Delta H1)}{8.314 \cdot T}$$

9. CALCULATE surface diffusivity

$$Ds2 := \frac{1.62 \cdot 10^{-2}}{1 \cdot 10^4} \cdot 2.712 \cdot \frac{-0.45 \cdot (-\Delta H2)}{8.314 \cdot T}$$

$$Ps1_i := \frac{2 \cdot \varepsilon^2 \cdot \tau m \cdot (1 - \varepsilon) \cdot Ds1 \cdot \rho m \cdot f1}{0.7515 \cdot \tau \cdot 82.06 \cdot \frac{101325}{1 \cdot 10^6} \cdot T \cdot r_i \cdot \tau}$$

10. CALCULATE the permeability due to surface diffusion

$$Ps2_i := \frac{2 \cdot \varepsilon^2 \cdot \tau m \cdot (1 - \varepsilon) \cdot Ds2 \cdot \rho m \cdot f2}{0.9758 \cdot \tau \cdot 82.06 \cdot \frac{101325}{1 \cdot 10^6} \cdot T \cdot r_i \cdot \tau}$$

$$P1_i := Pvis1_i + Pk1_i + Ps1_i$$

11. CALCULATE the total permeability.

$$P2_i := Pvis2_i + Pk2_i + Ps2_i$$

TYPE P1i= and P2i= to view the results

Study of permeability of gas as a function of pressure

z1 :=

	0	1	2
0	0	0	0
1	"P / bar"	"z"	"f"
2	40	0.7732	6.18·10 ⁻⁵
3	42	0.7721	6.489·10 ⁻⁵
4	44	0.7702	6.798·10 ⁻⁵
5	46	0.7687	7.107·10 ⁻⁵
6	48	0.7661	7.416·10 ⁻⁵
7	50	0.7643	7.725·10 ⁻⁵
8	52	0.7614	8.034·10 ⁻⁵
9	54	0.7598	8.343·10 ⁻⁵
10	56	0.7576	8.652·10 ⁻⁵
11	58	0.7545	8.961·10 ⁻⁵
12	60	0.7515	9.27·10 ⁻⁵
13	62	0.7465	9.579·10 ⁻⁵
14	64	0.7424	9.888·10 ⁻⁵
15	66	0.7378	0.0001
16	68	0.7322	0.0001
17	70	0.7298	0.0001

1. INPUT z and f for CO2

z2 :=

	0	1	2
0	0	0	0
1	"P / bar"	"z"	"f"
2	40	0.9897	2.15·10 ⁻⁵
3	42	0.9882	2.2575·10 ⁻⁵
4	44	0.9873	2.365·10 ⁻⁵
5	46	0.9861	2.4725·10 ⁻⁵
6	48	0.9856	2.58·10 ⁻⁵
7	50	0.9842	2.6875·10 ⁻⁵
8	52	0.9813	2.795·10 ⁻⁵
9	54	0.9805	2.9025·10 ⁻⁵
10	56	0.9791	3.01·10 ⁻⁵
11	58	0.9773	3.1175·10 ⁻⁵
12	60	0.9758	3.225·10 ⁻⁵
13	62	0.9738	3.3325·10 ⁻⁵
14	64	0.9718	3.44·10 ⁻⁵
15	66	0.9698	3.5475·10 ⁻⁵
16	68	0.9678	3.655·10 ⁻⁵
17	70	0.9658	3.7625·10 ⁻⁵

2. INPUT z and f for CH4

i := 2,3..17

j := 0,1..2

3. INPUT range of data desired

$$k := 1, 2, \dots, 15$$

$$P_k := 40 + 2(k - 1)$$

$$T := 303$$

$$r := 0.2 \cdot 10^{-9}$$

$$\varepsilon := 0.603$$

$$\tau := 1.658$$

$$t_m := 0.1 \cdot 10^{-6}$$

$$\rho_m := 3040$$

$$M1 := 44.01$$

$$M2 := 16.043$$

$$\sigma_1 := 3.3$$

$$\sigma_2 := 3.88$$

$$\Omega_1 := 1.2988$$

$$\Omega_2 := 1.1361$$

$$\Delta H1 := -17116$$

$$\Delta H2 := -21000$$

$$\mu_1 := 2.6693 \cdot 10^{-5} \cdot \frac{\sqrt{M1 \cdot T}}{\sigma_1^2 \cdot \Omega_1} \cdot \frac{100}{1000}$$

$$\mu_2 := 2.6693 \cdot 10^{-5} \cdot \frac{\sqrt{M2 \cdot T}}{\sigma_2^2 \cdot \Omega_2} \cdot \frac{100}{1000}$$

$$P_{vis1, i, k} := \varepsilon \cdot \frac{(r)^2 \cdot \left(\frac{P_k + 1.2}{2} \right)}{8 \cdot \tau \cdot \mu_1 \cdot z_{i,1} \cdot 82.06 \cdot T \cdot \frac{1}{10^6}}$$

$$P_{vis2, i, k} := \varepsilon \cdot \frac{(r)^2 \cdot \left(\frac{P_k + 1.2}{2} \right)}{8 \cdot \tau \cdot \mu_2 \cdot z_{i,1} \cdot 82.06 \cdot T \cdot \frac{1}{10^6}}$$

$$Dk1 := \frac{2 \cdot \left(r - \frac{0.33 \cdot 10^{-9}}{2} \right) \cdot \sqrt{\frac{8 \cdot 8.314 \cdot 1000 T}{3.142 \cdot M1}}}{3}$$

4. **INPUT** range of operating pressure and the specified temperature

5. **INPUT** properties (pore size, porosity, tortuosity, membrane thickness and density) of membrane

6. **INPUT** properties (molecular weights, kinetic diameter, Lennard-Jones parameters and heat of adsorption) of CO2 and CH4

7. **CALCULATE** the viscosity of gas components

8. **CALCULATE** permeability of gas due to viscous diffusion

9. **CALCULATE** Knudsen diffusivity

$$Dk2 := \frac{2 \cdot \left(r - \frac{0.38 \cdot 10^{-9}}{2} \right) \cdot \sqrt{\frac{8 \cdot 8.314 \cdot 1000 T}{3.142 \cdot M2}}}{3}$$

$$Pk1_i := \frac{\varepsilon \cdot \left(\frac{1}{\frac{1}{1.723 \cdot 10^{-5}} + \frac{1}{Dk1}} \right)}{z1_{i,1} \cdot \tau \cdot 82.06 \cdot \frac{101325}{1 \cdot 10^6} \cdot T}$$

$$Pk2_i := \frac{\varepsilon \cdot \left(\frac{1}{\frac{1}{1.723 \cdot 10^{-5}} + \frac{1}{Dk2}} \right)}{z2_{i,1} \cdot \tau \cdot 82.06 \cdot \frac{101325}{1 \cdot 10^6} \cdot T}$$

$$Ds1 := \frac{1.62 \cdot 10^{-2}}{1 \cdot 10^4} \cdot 2.712 \cdot \frac{-0.45 \cdot (-\Delta H1)}{8.314 \cdot T}$$

$$Ds2 := \frac{1.62 \cdot 10^{-2}}{1 \cdot 10^4} \cdot 2.712 \cdot \frac{-0.45 \cdot (-\Delta H2)}{8.314 \cdot T}$$

$$Ps1_i := \frac{2 \cdot \varepsilon^2 \cdot tm \cdot (1 - \varepsilon) \cdot Ds1 \cdot \rho m \cdot z1_{i,2}}{z1_{i,1} \cdot \tau \cdot 82.06 \cdot \frac{101325}{1 \cdot 10^6} \cdot T \cdot r}$$

$$Ps2_i := \frac{2 \cdot \varepsilon^2 \cdot tm \cdot (1 - \varepsilon) \cdot Ds1 \cdot \rho m \cdot z2_{i,2}}{z2_{i,1} \cdot \tau \cdot 82.06 \cdot \frac{101325}{1 \cdot 10^6} \cdot T \cdot r}$$

$$P1_{i,k} := Pvis1_{i,k} + Pk1_i + Ps1_i$$

$$P2_{i,k} := Pvis2_{i,k} + Pk2_i + Ps2_i$$

10. **CALCULATE** permeability of gas due to Knudsen diffusion

11. **CALCULATE** surface diffusivity

12. **CALCULATE** permeability of gas due to surface diffusion

13. **CALCULATE** total permeability of gas as function of operating pressure

TYPE the respective permeability function to obtain the range of data and **USE EXCEL** to plot the graphs

Study of permeability of gas as a function of temperature

z1 :=

	0	1	2
0	"T"	"z"	"f"
1	30	0.7515	$6.18 \cdot 10^{-5}$
2	40	0.7623	$5.4075 \cdot 10^{-5}$
3	50	0.7754	$4.8667 \cdot 10^{-5}$
4	60	0.7912	$4.4612 \cdot 10^{-5}$
5	70	0.8021	$4.1425 \cdot 10^{-5}$
6	80	0.8134	$3.8836 \cdot 10^{-5}$
7	90	0.8322	$3.6679 \cdot 10^{-5}$
8	100	0.8435	$3.4845 \cdot 10^{-5}$
9	110	0.8544	$3.3261 \cdot 10^{-5}$
10	120	0.8621	$3.1875 \cdot 10^{-5}$
11	130	0.8724	$3.0649 \cdot 10^{-5}$
12	140	0.8833	$2.9554 \cdot 10^{-5}$
13	150	0.8954	$2.8569 \cdot 10^{-5}$
14	160	0.9033	$2.7676 \cdot 10^{-5}$
15	170	0.9132	$2.6862 \cdot 10^{-5}$
16	180	0.9244	$2.6116 \cdot 10^{-5}$
17	190	0.9354	$2.5429 \cdot 10^{-5}$
18	200	0.9473	$2.4793 \cdot 10^{-5}$
19	210	0.9565	$2.4203 \cdot 10^{-5}$
20	220	0.9623	$2.3653 \cdot 10^{-5}$
21	230	0.9711	$2.3139 \cdot 10^{-5}$
22	240	0.9812	$2.2657 \cdot 10^{-5}$

1. INPUT z and f for CO2

z2 :=

	0	1	2
0	"T"	"z"	"f"
1	30	0.9758	2.15·10 ⁻⁵
2	40	0.9762	1.8813·10 ⁻⁵
3	50	0.9773	1.6931·10 ⁻⁵
4	60	0.9781	1.552·10 ⁻⁵
5	70	0.9788	1.4412·10 ⁻⁵
6	80	0.9791	1.3511·10 ⁻⁵
7	90	0.9799	1.276·10 ⁻⁵
8	100	0.9806	1.2122·10 ⁻⁵
9	110	0.9817	1.1571·10 ⁻⁵
10	120	0.9825	1.1089·10 ⁻⁵
11	130	0.9843	1.0663·10 ⁻⁵
12	140	0.9854	1.0282·10 ⁻⁵
13	150	0.9876	9.9392·10 ⁻⁶
14	160	0.9892	9.6286·10 ⁻⁶
15	170	0.9913	9.3454·10 ⁻⁶
16	180	0.9945	9.0858·10 ⁻⁶
17	190	0.9964	8.8467·10 ⁻⁶
18	200	1.0031	8.6255·10 ⁻⁶
19	210	1.0098	8.4201·10 ⁻⁶
20	220	1.0134	8.2288·10 ⁻⁶
21	230	1.0187	8.0499·10 ⁻⁶
22	240	1.0205	7.8822·10 ⁻⁶

2. INPUT z and f for CH4

i := 1,2..22

3. INPUT range of data desired

j := 0,1..2

k := 1,2..22

4. INPUT range of operating temperature and the specified pressure

$T_k := 30 + 10(k - 1)$

P := 60

$r := 0.2 \cdot 10^{-9}$

$\epsilon := 0.603$

5. INPUT properties (pore size, porosity, tortuosity, membrane thickness and density) of membrane

$\tau := 1.658$

$tm := 0.1 \cdot 10^{-6}$

$\rho_m := 3040$

M1 := 44.01

6. INPUT properties (molecular weights, kinetic diameter, Lennard-Jones parameters and heat of adsorption) of CO2 and CH4

M2 := 16.043

$\sigma_1 := 3.3$

$\sigma_2 := 3.88$

$\Omega_1 := 1.2988$

$\Omega_2 := 1.1361$

$$\Delta H1 := -17116$$

$$\Delta H2 := -21000$$

$$\mu_{1k} := 2.6693 \cdot 10^{-5} \cdot \frac{\sqrt{M1 \cdot (T_k + 273)}}{\sigma_1^2 \cdot \Omega_1} \cdot \frac{100}{1000}$$

7. **CALCULATE** the viscosity of gas components

$$\mu_{2k} := 2.6693 \cdot 10^{-5} \cdot \frac{\sqrt{M2 \cdot (T_k + 273)}}{\sigma_2^2 \cdot \Omega_2} \cdot \frac{100}{1000}$$

$$Pvis1_{i,k} := \varepsilon \cdot \frac{(r)^2 \cdot \left(\frac{P + 1.2}{2}\right)}{8 \cdot \tau \cdot \mu_{1k} \cdot z_{1,i,1} \cdot 82.06 \cdot (T_k + 273)} \cdot \frac{1}{10^6}$$

8. **CALCULATE** permeability of gas due to viscous diffusion

$$Pvis2_{i,k} := \varepsilon \cdot \frac{(r)^2 \cdot \left(\frac{P + 1.2}{2}\right)}{8 \cdot \tau \cdot \mu_{2k} \cdot z_{2,i,1} \cdot 82.06 \cdot (T_k + 273)} \cdot \frac{1}{10^6}$$

$$Dk1_k := \frac{2 \cdot \left(r - \frac{0.33 \cdot 10^{-9}}{2}\right) \cdot \sqrt{\frac{8 \cdot 8.314 \cdot 1000 \cdot (T_k + 273)}{3.142 \cdot M1}}}{3}$$

9. **CALCULATE** Knudsen diffusivity

$$Dk2_k := \frac{2 \cdot \left(r - \frac{0.38 \cdot 10^{-9}}{2}\right) \cdot \sqrt{\frac{8 \cdot 8.314 \cdot 1000 \cdot (T_k + 273)}{3.142 \cdot M2}}}{3}$$

$$Pk1_{i,k} := \frac{\varepsilon \cdot \left(\frac{1}{\frac{1}{1.723 \cdot 10^{-5}} + \frac{1}{Dk1_k}}\right)}{z_{1,i,1} \cdot \tau \cdot 82.06 \cdot \frac{101325}{1 \cdot 10^6} \cdot (T_k + 273)}$$

10. **CALCULATE** permeability of gas due to Knudsen diffusion

$$Pk2_{i,k} := \frac{\varepsilon \cdot \left(\frac{1}{\frac{1}{1.723 \cdot 10^{-5}} + \frac{1}{Dk2_k}}\right)}{z_{2,i,1} \cdot \tau \cdot 82.06 \cdot \frac{101325}{1 \cdot 10^6} \cdot (T_k + 273)}$$

$$Ds1_k := \frac{1.62 \cdot 10^{-2}}{1 \cdot 10^4} \cdot 2.712 \cdot \frac{-0.45 \cdot (-\Delta H1)}{8.314 \cdot (T_k + 273)}$$

11. **CALCULATE** surface diffusivity

$$Ds2_k := \frac{1.62 \cdot 10^{-2}}{1 \cdot 10^4} \cdot 2.712 \cdot \frac{-0.45 \cdot (-\Delta H2)}{8.314 \cdot (T_k + 273)}$$

$$Ps1_{i,k} := \frac{2 \cdot \varepsilon^2 \cdot tm \cdot (1 - \varepsilon) \cdot Ds1_k \cdot \rho m \cdot z1_{i,2}}{z1_{i,1} \cdot \tau \cdot 82.06 \cdot \frac{101325}{1 \cdot 10^6} \cdot (T_k + 273) \cdot r\tau}$$

$$Ps2_{i,k} := \frac{2 \cdot \varepsilon^2 \cdot tm \cdot (1 - \varepsilon) \cdot Ds2_k \cdot \rho m \cdot z2_{i,2}}{z2_{i,1} \cdot \tau \cdot 82.06 \cdot \frac{101325}{1 \cdot 10^6} \cdot (T_k + 273) \cdot r\tau}$$

12. **CALCULATE** permeability of gas due to surface diffusion

$$P1_{i,k} := Pvis1_{i,k} + Pk1_{i,k} + Ps1_{i,k}$$

$$P2_{i,k} := Pvis2_{i,k} + Pk2_{i,k} + Ps2_{i,k}$$

13. **CALCULATE** total permeability of gas as function of operating temperature

TYPE the respective permeability function to obtain the range of data and **USE EXCEL** to plot the graphs

Study to determine the separation factor

$$y := 0.2$$

$$x := 0.2 \quad \text{initial guess for y and x}$$

Given

$$x = \frac{0.25 - 0.206 \cdot y}{1 - 0.206} \quad (\text{Equation 1})$$

$$\frac{y}{1 - y} - \frac{6.6 \cdot (x - 0.017 \cdot y)}{(1 - x) - 0.017 \cdot (1 - y)} = 0.00001 \quad (\text{Equation 2})$$

$$\begin{pmatrix} \text{xval} \\ \text{yval} \end{pmatrix} := \text{Find}(x, y)$$

$$\begin{pmatrix} \text{xval} \\ \text{yval} \end{pmatrix} = \begin{pmatrix} 0.169 \\ 0.561 \end{pmatrix} \quad \underline{\text{Answers obtained when equation 2 is satisfied. Use Excel to study the separation factor.}}$$